Fluid and particle signatures of dayside reconnection

T. M. Bauer, G. Paschmann, N. Sckopke, R. A. Treumann, W. Baumjohann, T.-D. Phan

Annales Geophysicae (2001) 19: 1045–1063 © European Geophysical Society 2001

Annales Geophysicae

Fluid and particle signatures of dayside reconnection

T. M. Bauer[1], **G. Paschmann**[1,2], **N. Sckopke**[1,*], **R. A. Treumann**[1,2,3], **W. Baumjohann**[1,4], **and T.-D. Phan**[5]

[1]Max-Planck-Institut für extraterrestrische Physik, Garching, Germany
[2]International Space Science Institute, Bern, Switzerland
[3]Centre for Interdisciplinary Plasma Science, Garching, Germany
[4]Institut für Weltraumforschung der Österreichischen Akademie der Wissenschaften, Graz, Austria
[5]Space Sciences Laboratory, University of California, Berkeley
[*]Deceased 28 November 1999

Received: 20 October 2000 – Revised: 15 May 2001 – Accepted: 13 June 2001

Abstract. Using measurements of the AMPTE/IRM spacecraft, we study reconnection signatures at the dayside magnetopause. If the magnetopause is open, it should have the properties of a rotational discontinuity. Applying the fluid concept of a rotational discontinuity, we check for the existence of a de Hoffmann-Teller frame and the tangential stress balance (Walén relation). For 13 out of 40 magnetopause crossings in a statistical survey we find a reasonable agreement between observed plasma flows and those predicted by the Walén relation. In addition, we check if the measured distribution functions show single particle signatures which are expected on open field lines. We find the following types of signatures: field-aligned streaming of ring current particles, "D-shaped" distributions of solar wind particles, counterstreaming of solar wind and cold ionospheric ions, two-beam distributions of solar wind ions, and distributions of solar wind particles associated with field-aligned heat flux. While a particular type of particle signature is observed only for the minority of magnetopause crossings, 24 of the 40 crossings show at least one type of signature. Both the particle signatures and the fit to the Walén relation can be used to infer the sign of the normal magnetic field, B_n. We find that the two ways of inferring the sign of B_n lead primarily to the same result. Thus, both the particle signatures and a reasonable agreement with the Walén relation can, in a statistical sense, be considered as a useful indicator of open field lines. On the other hand, many crossings do not show any reconnection signatures. We discuss the possible reasons for their absence.

Key words. Magnetopause, cusp and boundary layers; magnetosheath; solar wind – magnetosphere interactions

1 Introduction

Immediately earthward of the magnetopause at low-latitudes there is a boundary layer commonly populated by shocked solar wind plasma from the magnetosheath and magnetospheric plasma. Since its discovery (Eastman et al., 1976), the formation of the low-latitude boundary layer, i.e. the entry of solar wind plasma onto geomagnetic field lines earthward of the magnetopause is one of the outstanding problems of magnetospheric physics. It is now widely believed that magnetic reconnection (Dungey, 1961) is the dominant entry mechanism. After reconnection has produced a finite normal magnetic field B_n across the magnetopause, plasma can cross the magnetopause along open field lines. Since direct measurements of B_n are difficult, the most important evidence for reconnection at the magnetopause is provided indirectly by observations of accelerated bulk plasma flows, first reported by Paschmann et al. (1979) in agreement with model predictions, by observation or inference of field-aligned electron beams (Ogilvie et al., 1984; Pottelette and Treumann, 1998), and by observations of the single particle signatures (e.g. Fuselier et al., 1991, 1995; Nakamura et al., 1996) expected on open field lines (Cowley, 1982).

If the magnetopause is time stationary and tangential gradients are small compared to normal gradients, the magnetopause can be modeled as a magnetohydrodynamic discontinuity. A magnetically closed ($B_n = 0$) magnetopause can be modeled as a tangential discontinuity, while a magnetically open ($B_n \neq 0$) magnetopause can be modeled as a rotational discontinuity. In both cases, the magnetopause is assumed to be infinitely thin. The measured time series of macroscopic plasma moments can, in principle, (and with some caution; see Scudder, 1997) be used to check for the existence of a de Hoffmann-Teller frame, as well as the tangential stress balance. The condition of thinness of the discontinuity requires that the plasma moments are measured sufficiently far outside of the discontinuity, where the single-fluid magnetohydrodynamic approximation is valid. However, experience has shown that for sufficiently flat plasma and field gradients, an approximate use of plasma moments is justified also inside the transition. This holds, in particular, for rotational discontinuities where plasma flows across the boundary and fills a certain region inside of the discontinuity, thereby flattening the plasma and field gradients. It is clear

Correspondence to: R. A. Treumann (tre@mpe.mpg.de)

that the discontinuity in such a case looses its strict magnetohydrodynamic properties; it becomes a two-fluid transition or assumes the character of a kinetic transition layer. In the presence of strong transverse diffusion, the same argument applies to a tangential discontinuity. The properties of the transitions in both of these cases will, however, conserve a taste of their origin. They can, in many cases, still be distinguished by observing the typical characteristics of tangential and rotational discontinuities when applying the conditions at these discontinuities in a statistical sense to the moments measured across the transition layer. This is particularly reasonable when the errors of the measurement of the moments cannot be neglected and when there are no distinctive measurements of the different particle species available, as in the cases communicated in the present paper. Of course, precise knowledge of the ionic particle composition (e.g. Puhl-Quinn and Scudder, 2000) and measurement of the electron flow velocity $\mathbf{V}_e$ would be desirable. The latter directly yields the electric convection field across the boundary layer from the condition $\mathbf{E} = -\mathbf{V}_e \times \mathbf{B}$ (see, e.g. Scudder, 1997; Baumjohann and Treumann, 1997). Such measurements must await the success of the plasma-gun experiment scheduled for the CLUSTER mission. Meanwhile, in this paper, we restrict ourselves to the achievable and analyze the plasma measurements of the AMPTE/IRM spacecraft when it crosses the magnetopause. In this case, one is restricted to taking the measured ion bulk flow velocity as a proxy. The distinction between the two types of discontinuities is then approximately accomplished by trying to determine the typical average de Hoffmann-Teller frame of reference.

The de Hoffmann-Teller frame is a frame moving at velocity $\mathbf{V}_{\rm HT}$ in which the transformed plasma bulk velocity, $\mathbf{V}' = \mathbf{V} - \mathbf{V}_{\rm HT}$, is purely field-aligned and, therefore, the convection electric field, $\mathbf{E}'_c = -\mathbf{V}' \times \mathbf{B}$, vanishes. A rotational discontinuity should have an approximate de Hoffmann-Teller frame, whereas a tangential discontinuity does, in general, not have such a frame if the discontinuity is actually resolved in the measurements (Sonnerup et al., 1987, 1990). $\mathbf{E}'_c = 0$ can be used to estimate the average de Hoffmann-Teller velocity, $\mathbf{V}_{\rm HT}$, along the presumptive discontinuity of an observed magnetopause from the measured time series of the proton bulk velocity, $\mathbf{V}_p$, and the magnetic field, $\mathbf{B}$. Hereby, $\mathbf{V}_{\rm HT}$ is obtained as the vector that minimizes the quadratic form

$$D = \langle |(\mathbf{V}_p - \mathbf{V}_{\rm HT}) \times \mathbf{B}|^2 \rangle \tag{1}$$

which is approximately the square of $\mathbf{E}'_c$ averaged over measurements taken in the vicinity of the magnetopause (Sonnerup et al., 1987). If the minimum of D is well-defined and the estimated convection electric field, $\mathbf{E}_c = -\mathbf{V}_p \times \mathbf{B}$, is approximately equal to the transformation electric field, $\mathbf{E}_{\rm HT} = -\mathbf{V}_{\rm HT} \times \mathbf{B}$, we can conclude that within the approximations and restrictions discussed above, a de Hoffmann-Teller frame exists for the magnetopause crossing under consideration. Strictly speaking, the quality of the de Hoffmann-Teller velocity and frame determined in this way should be checked, even in the case of the availability of the electron bulk flow, by methods such as a χ^2-test in order to find out to what degree the measurement supports the interpretation of the obtained velocity as attributed to a frame moving with de Hoffmann-Teller speed along the rotational discontinuity. This test does not many any sense in our approximate case, as it is clear from the above argument that the discontinuity is only an approximation. and that the constructed de Hoffmann-Teller frame will only hold in a very average sense, merely serving as a rough distinction between cases when the magnetopause/low-latitude boundary layer system is approximately open or closed. Since it must be expected that diffusive processes over the entire magnetopause surface cause considerably slower plasma and field diffusion than for reconnection, such a distinction will make sense and can contribute valuable information about the properties of the magnetopause and boundary layer in both cases, even when holding only approximately.

Similar arguments apply when using the tangential stress balance (Walén relation) of a rotational discontinuity as an additional argument for distinguishing between open and closed magnetopause conditions. The ideal way would be to base the Walén test on electron flow measurements, as was done by Scudder et al. (1999). Since we are restricted to bulk flow measurements with no resolution of the composition (see, e.g. Puhl-Quinn and Scudder, 2000), our tests will hold in the average sense as discussed above. The Walén relation in this case states that the plasma bulk velocity in the de Hoffmann-Teller frame is approximately Alfvénic. Again, and as stated above, by replacing the plasma bulk velocities, $\mathbf{V}$ and $\mathbf{V}'$, with the proton bulk velocities, $\mathbf{V}_p \approx \mathbf{V}$ and $\mathbf{V}'_p \approx \mathbf{V}'$, this condition reads

$$\mathbf{V}'_p = \mathbf{V}_p - \mathbf{V}_{\rm HT} = \pm \mathbf{c}_A = \pm \frac{\mathbf{B}(1-\alpha)^{1/2}}{(\mu_0 N m_p)^{1/2}} \tag{2}$$

where $\mathbf{c}_A$ is the Alfvén velocity in a plasma with number density N and pressure anisotropy $\alpha = (P_\parallel - P_\perp)\mu_0/B^2$. The latter is defined as the difference between the plasma pressures parallel and perpendicular to $\mathbf{B}$ divided by twice the magnetic pressure, $P_B = B^2/2\mu_0$. The $+$ sign ($-$ sign) is valid when the normal component V_{pn} of the proton bulk flow has the same (opposite) direction as B_n. Scudder et al. (1999) and Puhl-Quinn and Scudder (2000) have shown that when this method is used in the absence of available electron flux, it will still lead to an approximate correlation, but that the numerical coefficient of this correlation will be incorrect. Hence, in view of this result, the inference will be qualitative, which for our purposes, here, is sufficient.

Sonnerup et al. (1987, 1990), and Paschmann et al. (1990) checked the fit between the data and the prediction of Eq. (2) by producing a single scatter plot of $\mathbf{V}'_p$ versus $\mathbf{c}_A$, in which all three Cartesian components are plotted together. The fit was then quantified by computing the correlation coefficient C^*_{V',c_A} of this plot and the slope Λ^*_{V',c_A} of its regression line. For the magnetopause crossings analyzed in this paper, we compute, in addition, the quantities C_{V,c_A} and $V'_{p\parallel}/c_A$. The ratio $V'_{p\parallel}/c_A$ is evaluated for each measurement of the field-aligned component of $\mathbf{V}'_p$ and the Alfvén speed. C_{V,c_A} is

the cross-correlation of the components of $\mathbf{V}_p$ and $\mathbf{c}_A$ along the maximum variance direction of $\mathbf{B}$, $\mathbf{B}$ (Sonnerup et al., 1987) which is tangential to the magnetopause and it is chosen, because it is approximately the direction along which the variation of $\mathbf{c}_A$ has the highest dynamic range. If C_{V,c_A}, $V'_{p\|}/c_A$, C^*_{V',c_A}, and Λ^*_{V',c_A} are all close to $+1$ (-1), then the data agree with the prediction for a rotational discontinuity with $B_n < 0$ ($B_n > 0$). Across a tangential discontinuity the variation of $\mathbf{V}$ does not depend on the variation of $\mathbf{c}_A$. Therefore, C_{V,c_A} can assume arbitrary values in the case of a closed magnetopause, and the other three quantities cannot be defined if a de Hoffmann-Teller frame does not exist.

The quality of the de Hoffmann-Teller frame is checked by producing a scatter plot of $\mathbf{E}_c$ versus $\mathbf{E}_{\rm HT}$ (Sonnerup et al., 1987, 1990; Paschmann et al., 1990). Then the fit is quantified by computing the correlation coefficient $C^*_{E_c,E_{\rm HT}}$ of this plot and the slope $\Lambda^*_{E_c,E_{\rm HT}}$ of its regression line. In addition, we compute the cross correlation $C_{E_c,E_{\rm HT}}$ of the components $\mathbf{E}_c$ and $\mathbf{E}_{\rm HT}$ along the maximum variance direction of $\mathbf{E}_c$ and the slope $\Lambda_{E_c,E_{\rm HT}}$ of their common regression line.

If the plasma moments measured during a magnetopause crossing determine a well-defined de Hoffmann-Teller frame and are in reasonable agreement with the Walén relation (2), we say that the respective crossing shows the fluid signature of magnetic reconnection. At the dayside magnetopause, accelerated plasma flows in good agreement with Eq. (2) were detected by the ISEE satellites (Paschmann et al., 1979; Sonnerup et al., 1981; Gosling et al., 1990a), the AMPTE/UKS spacecraft (Johnstone et al., 1986), and the AMPTE/IRM spacecraft (Sonnerup et al., 1987, 1990; Paschmann et al., 1986, 1990). Recently, Phan et al. (2000) succeeded in observing the accelerated flows simultaneously north ($B_n < 0$) and south ($B_n > 0$) of the X-line with the Equator-S and Geotail spacecrafts, respectively.

In the previous investigations, a good regression of $\mathbf{V}'_p$ versus $\mathbf{B}$ was often found to exist, although its slope, $\Lambda^*_{E_c,E_{\rm HT}}$, was substantially different from the value 1 (-1) predicted for a rotational discontinuity. In these studies and also in ours, the data are compared with the predictions of ideal magnetohydrodynamics (MHD). Moreover, the plasma bulk velocity is approximated by the proton bulk velocity. Scudder (1997), Scudder et al. (1999), and Puhl-Quinn and Scudder (2000) demonstrated that the MHD description becomes inaccurate in the presence of strong electric currents and that a more reliable test of the predictions for a rotational discontinuity can be performed by comparing magnetic field changes with changes in the electron bulk velocity, $\mathbf{V}_e$. We cannot take this approach, since the electron bulk velocity measured by AMPTE/IRM is too inaccurate due to an instrumental defect (Appendix 1 of Paschmann et al., 1986).

Particle distribution functions expected at an open magnetopause have been described by Cowley (1982). After reconnection has produced a finite B_n, ring current and ionospheric particles can move outward, i.e. toward the solar wind end of an open field line, and solar wind particles can move inward, i.e. toward its terrestrial end. If the magnetopause current layer is sufficiently thin, the ion motion in the current layer becomes non-adiabatic. Then an ion component incident on the current layer is only partly transmitted; the other part is reflected. For reflection at a thin current layer the field-aligned flow velocities in the de Hoffmann-Teller frame of the reflected ($V'_{r\|}$) and incident ($V'_{i\|}$) component fulfill $V'_{r\|} = -V'_{i\|}$. In the de Hoffmann-Teller frame, the particle velocities $\mathbf{v}'$ of inward moving particles fulfill $v'_\| > 0$ when B_n points inward, and $v'_\| < 0$ when B_n points outward. For outward moving particles, it is the other way round. Hence, each component of the incident, reflected, and transmitted plasma populations should have a velocity cutoff at $v'_\| = 0$. Distribution functions with such a velocity cutoff are called "D-shaped" distributions and were observed by Gosling et al. (1990b), Smith and Rodgers (1991), Fuselier et al. (1991), and Nakamura et al. (1997). Ion reflection off the magnetopause was reported by Sonnerup et al. (1981), Gosling et al. (1990a), and Fuselier et al. (1991). It should be noted that only close to the magnetopause does the velocity cutoff appear at $v'_\| = 0$. Farther away from the magnetopause, the velocity filtering leads to a different cutoff (e.g. Nakamura et al., 1996, 1998).

The previous case studies of magnetopause crossings found not only cases in agreement with the reconnection model, but also many cases that show no fluid or particle signatures of reconnection, i.e the measured plasma moments do not agree with Eq. (2) and the distribution functions do not show the signatures predicted by Cowley (1982). In these cases, it must be concluded that the local magnetopause is closed. Phan et al. (1996) performed a survey of all AMPTE/IRM crossings in the local time (LT) range of 08:00–16:00 with high ($> 45°$) magnetic shear across the magnetopause. They found that 61% of the crossings showed a reasonable agreement with the Walén relation.

In this paper, we use the AMPTE/IRM data to perform a combined survey of both the fluid and particle signatures at the dayside magnetopause. Using different criteria than Phan et al. (1996), we reexamine how often a reasonable agreement with the Walén relation is observed. In addition, we address the following questions: how often are the different types of particle signatures observed? Do all events with particle signatures also show a reasonable agreement with the Walén relation or is it the other way around? In Sect. 3, four magnetopause passes are analyzed in detail. In Sects. 5 to 7 we will present the statistical survey of reconnection signatures. A statistical analysis of the plasma populations in the sublayers of the boundary layer and of the average time profiles will be provided in a companion paper (Bauer et al., 2000, hereafter referred to as paper 2).

2 Instrumentation

We use measurements of the triaxial flux gate magnetometer (Lühr et al., 1985), and the plasma instrument on board the IRM spacecraft. The plasma instrument (Paschmann et al., 1985) consists of two electrostatic analyzers of the top hat type, one for ions and one for electrons. Three-dimensional

distributions with 128 angles and 30 energy channels in the energy-per-charge range from 15 V to 30 kV for electrons, and 20 V to 40 kV for ions were obtained for every satellite rotation period, i.e. every 4.4 s. From each distribution, microcomputers within the instruments computed moments of the distribution functions of ions and electrons: densities in three contiguous energy bands: the bulk velocity vector, the pressure tensor, and the heat flux vector. In these computations it was assumed that all the ions were protons. Whereas the moments were transmitted to the ground at the full time resolution, the distributions themselves were transmitted less frequently because the allocated telemetry was limited. For this paper, we use magnetic field data averaged over the satellite rotation period.

3 Case studies

In this section, four magnetopause passes of AMPTE/IRM are analyzed in detail. We use measurements taken by the magnetometer (Lühr et al., 1985) and the plasma instrument (Paschmann et al., 1985) on board IRM. A short description of these instruments is given in paper 2. The magnetic field and the proton bulk velocity are displaced in LMN boundary normal coordinates (Russell and Elphic, 1979). The magnetopause normal, **n**, is taken from the model of Fairfield (1971) and points outward. For the magnetopause crossings examined in Sects. 3.1 and 3.2, the shear between the magnetic fields in the magnetosheath and in the boundary layer is high ($|\Delta\varphi_B| > 90°$). The crossings examined in Sects. 3.3 and 3.4 are low shear crossings ($|\Delta\varphi_B| < 30°$).

3.1 Crossing on 21 September 1984

Figure 1 presents an overview of the outbound magnetopause crossing on 21 September 1984, which occured at $13°$ northern GSM latitude at 11:10 LT. The magnetopause at 13:01:11 UT can be identified as a rotation of the magnetic field tangential to the magnetopause: φ_B changes by about $90°$. After 13:01:11, IRM is located in the magnetosheath. Earthward of the magnetopause three different regions can be distinguished. From ∼12:57 to 12:58:51, the IRM is in the magnetosphere proper and from 13:01:02 to 13:01:11, it is located in the outer boundary layer (OBL), a region of dense magnetosheath-like plasma. The duration of this OBL is relatively short. As we will see in Sects. 3.3 and 4, there are crossings for which the OBL lasts considerably longer. Before ∼12:57 and during the intervals 12:58:51–13:00:01 and 13:00:18–13:01:02, the total density is somewhat higher than in the magnetosphere proper and the contribution of solar wind particles to the density is comparable to the contribution of magnetospheric particles. We call this region the inner boundary layer (IBL). In the plasma moments of Fig. 1, the difference between the IBL and the magnetosphere is hard to see, but it will become clearly visible in the distributions. The division of the boundary layer into an outer and inner part was already reported by Sckopke et al. (1981) and Fujimoto et al. (1998) for the flanks, as well as by Hapgood and Bryant (1990), Hall et al. (1991), Song et al. (1993), and Le et al. (1996) for the dayside magnetopause. The enhancement of N_e and depression of T_p, T_e around 13:00:10 correspond to a flux transfer event (FTE). It exhibits the $+-$ bipolar signature of B_n (not shown) expected for open magnetic flux tubes moving northward (e.g. Cowley, 1982).

In the panel of V_{pL}, we recognize a northward directed reconnection flow in the OBL. The interval between 13:01:02 and 13:01:28 around the magnetopause suggests that a de Hoffmann-Teller frame ($C_{E_c,E_{\rm HT}} = 0.86$, $\Lambda_{E_c,E_{\rm HT}} = 0.97$) exists. The time series of $\mathbf{V}_p$ and $\mathbf{c}_A$ are correlated. The cross-correlation coefficient C_{V,c_A} of the components along the maximum variance direction of **B** equals $+0.9$. The sign of C_{V,c_A} indicates $B_n < 0$, i.e. open field lines connected to the northern hemisphere.

Panel a of Fig. 2 presents a series of electron distributions measured on 21 September 1984 in the magnetosphere (12:58:32), the IBL (13:00:21), the OBL (13:01:05), and the magnetosheath (13:01:48). In the magnetosheath, the IRM detects solar wind electrons with thermal energy $KT \approx 50\,\mathrm{eV}$. The distribution taken in the magnetosphere proper at 12:58:32 shows hot ($KT \approx 5\,\mathrm{keV}$) ring current electrons at velocities $v > 10\,000\,\mathrm{km/s}$ and cold ($KT \sim 10\,\mathrm{eV}$) electrons, presumably of ionospheric origin at velocities $v < 4000\,\mathrm{km/s}$.

From the sign of C_{V,c_A}, we inferred that the local magnetopause has an inward directed normal magnetic field, $B_n < 0$. This result is strongly supported by the electron distribution taken in the OBL at 13:01:05. We see solar wind electrons streaming parallel to **B** (inward along open field lines) and simultaneously hot ring current electrons streaming antiparallel to **B** (outward). In a plot of phase space density rather than energy flux density, the solar wind population would have the "D shape" predicted by Cowley (1982). In the IBL at 13:00:21, the IRM detects hot ring current electrons and another population at field-aligned velocities $v_\parallel \approx 8000\,\mathrm{km/s}$. This population was already observed by the ISEE satellites (Ogilvie et al., 1984) and by AMPTE-UKS (Hall et al., 1991), and was called "counterstreaming" electrons. Since this nomenclature might be taken to imply a balance between the fluxes parallel and antiparallel to **B**, we prefer to call it "warm" electrons. The term "warm" shall indicate that the field-aligned temperature of this population is primarily higher than that of solar wind electrons in the magnetosheath and in the OBL. The origin of the warm electrons will be discussed in paper 2.

Let us turn to the series of ion distributions (Fig. 2b) obtained in the magnetosphere (12:58:18), the IBL (13:00:34), the OBL (13:01:05), and the magnetosheath (13:01:39). As expected on open field lines with $B_n < 0$, the distributions in the magnetosheath and in the OBL show solar wind ion plasma with the flow velocity $\mathbf{V}'$ in the de Hoffmann-Teller frame parallel to **B**. The distribution in the OBL has the characteristic "D shape" predicted by Cowley (1982). Its cutoff velocity is consistent with $\mathbf{V}_{\rm HT}$: there are only a few ions with field-aligned particle velocities $v'_\parallel < 0$. Checking the

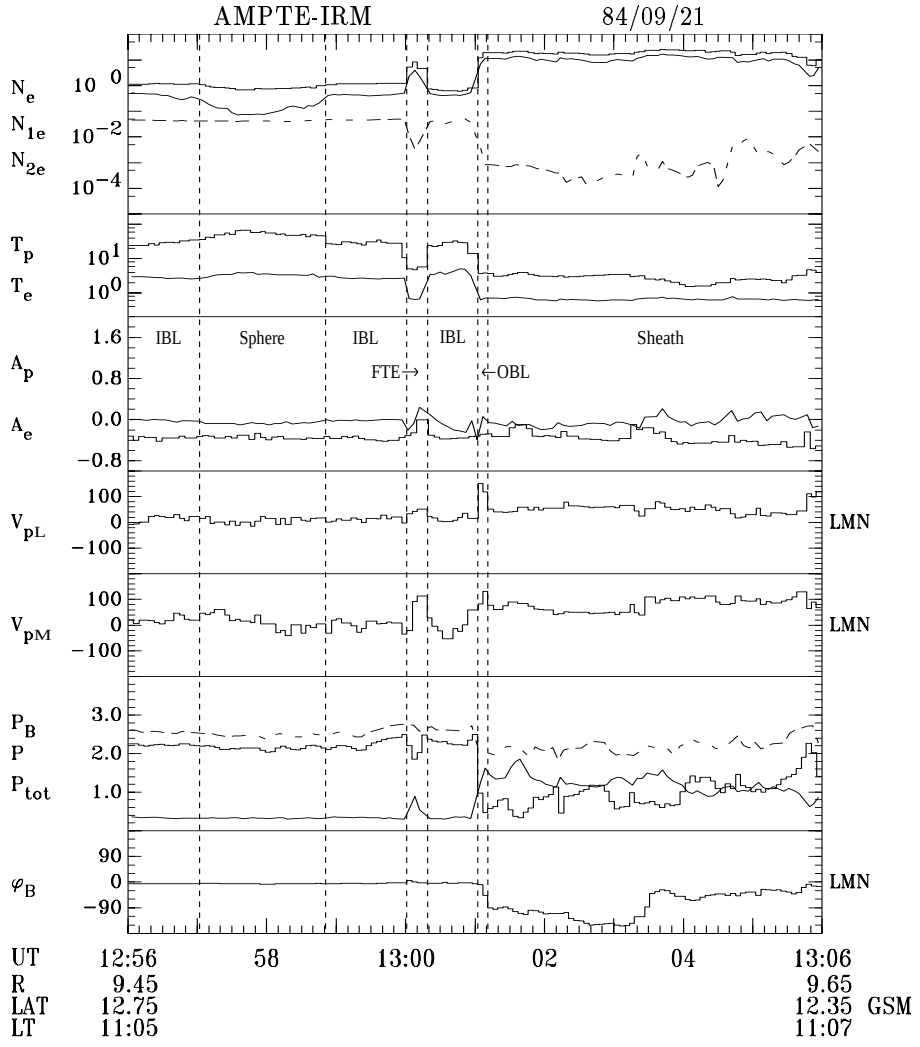

Fig. 1. Overview of the magnetopause pass on 21 September 1984. The upper panel shows the total (15 eV–30 keV) electron density, N_e (histogram line), in cm^{-3} and the partial densities, N_{1e} (solid line) and N_{2e} (dashed line), of electrons in the energy ranges 60 eV–1.8 keV and 1.8 keV–30 keV, respectively. In the next two panels, the proton and electron temperatures, T_p (histogram line) and T_e (solid line), in 10^6 K and the respective anisotropies, $A_p = T_{p\parallel}/T_{p\perp} - 1$ (histogram line) and $A_e = T_{e\parallel}/T_{e\perp} - 1$ (solid line), are given. The next two panels present the components V_{pL} and V_{pM} of the proton bulk velocity in km/s. V_{pL} and V_{pM} refer to the boundary normal coordinate system. In the sixth panel, the magnetic pressure, P_B (histogram line), plasma pressure, $P = N_pKT_p + N_eKT_e$ (solid line), and total pressure, $P_{\mathrm{tot}} = P_B + P$ (dashed line), in nPa are shown. The last panel gives the angle φ_B the magnetic field makes with the L axis in the LM plane of the boundary normal coordinate system. Vertical dashed lines indicate boundaries separating different plasma regions.

ratio $V'_{p\parallel}/c_A$ of the field-aligned proton bulk velocity in the de Hoffmann-Teller frame and the Alfvén speed, we find that it is $+0.2$ in the magnetosheath and $+0.5$ in the OBL, which differs considerably from the value $+1$ predicted by Eq. (2). Nevertheless, the ion and electron distributions observed in the OBL provide evidence for the OBL on open field lines with $B_n < 0$.

In the limited energy range shown in Fig. 2b, no ions are measured in the magnetosphere proper. However, in Fig. 3, which displays the whole energy range of the plasma instrument, we observe that the IRM detects hot ring current ions with thermal energy $KT \approx 10\,\mathrm{keV}$ at velocities $v > 1000\,\mathrm{km/s}$. These are also detected in the IBL, OBL, and magnetosheath. The ring current ions in the magnetosheath could be taken as further evidence for an open magnetopause with $B_n < 0$: their streaming antiparallel to **B** suggests that they escape to the magnetosheath along open field lines. However, this conclusion may be ambiguous as a very thin current layer allows energetic particles of large gyro-radii to escape from the magnetosphere as well.

Apart from the ring current population, the distributions taken in the IBL after the passage of the FTE (see the one given in Fig. 2b) show solar wind ions ($KT \sim 1\,\mathrm{keV}$), whereas before the FTE, cold ($KT \sim 10\,\mathrm{eV}$) ions of ionospheric origin are detected instead. The electron distributions measured before and after the FTE are similar to one another. For many of the distributions taken in the IBL, e.g. for the one given in Fig. 2b, the proton bulk velocity $\mathbf{V}'_p$ in the de Hoffmann-Teller frame has a substantial component perpendicular to **B**. This can be taken as an argument that the IBL is not located on open field lines crossing the OBL. Information about the IBL can also be deduced from the time series of N_{2e} and V_{pM}. In the IBL, the partial density N_{2e} of electrons above 1.8 keV has about the same value as in the magnetosphere proper, but it drops at the interface between the IBL and the OBL. Such a drop is expected at the boundary between closed and open field lines. In the OBL, V_{pM} is directed dawnward, as expected for plasma on tailward moving open field lines on the dawnside (11:10 LT). In contrast, V_{pM} is highly variable in the IBL before the FTE and even directed duskward after the FTE. These features taken together suggest that the IBL is on closed field lines.

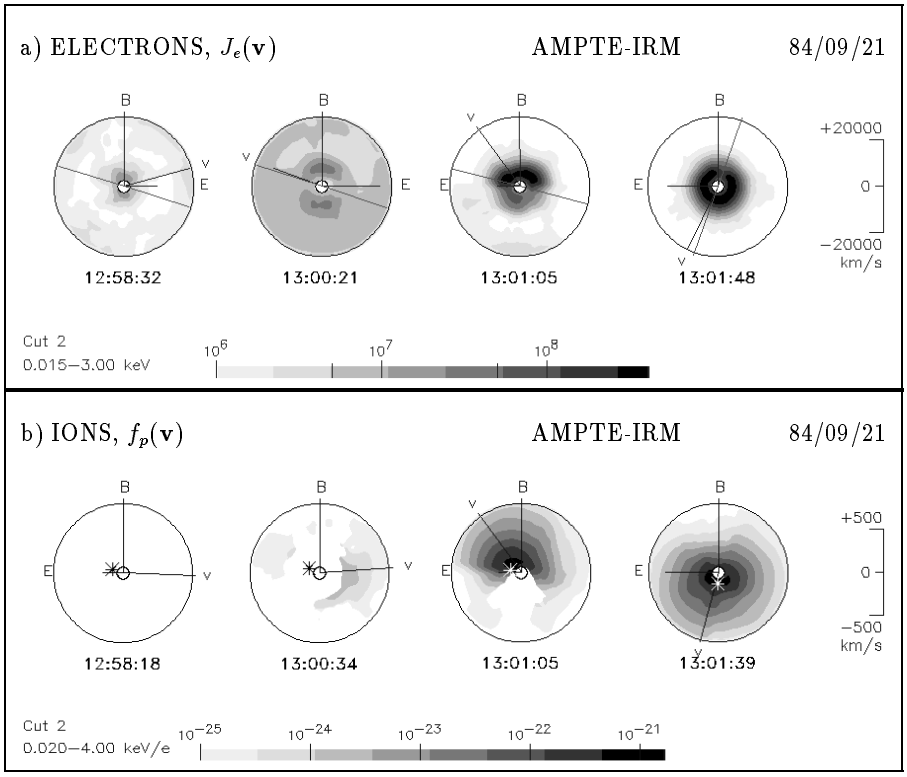

Fig. 2. Ion distributions in the energy range of 20 eV–4 keV and electron distributions in the range of 15 eV–3 keV measured on 21 September 1984. Panel a shows the differential directional energy flux density J_e (in $\mathrm{eV/s\,cm^2 eV\,sr}$) of electrons. Panel b shows the phase space density f_p (in $\mathrm{cm^{-6}\,s^3}$) of ions. The distributions are shown in a two-dimensional cut through velocity space in the spacecraft frame that contains the magnetic field direction, **B** (upward), and $\mathbf{n} \times \mathbf{B}$ (to the left), where **n** is the magnetopause normal. Moreover, projections of the directions of the proton bulk flow, $\mathbf{V}_p$, and the convection electric field, $\mathbf{E}_c = -\mathbf{V}_p \times \mathbf{B}$, are given. Black or white stars in the ion distributions give the projection of the de Hoffmann-Teller velocity, $\mathbf{V}_{\mathrm{HT}}$, onto the cut. $\mathbf{V}_{\mathrm{HT}}$ is determined by the minimization of D (Eq. 1) and is the origin of the $\mathbf{v}'$ system used in the text. In the electron distributions there is another line which is symmetric about $v = 0$. This line gives the projection of the IRM spin axis. Due to an instrumental defect, some distributions exhibit a reduced electron flux along the spin axis at low energies.

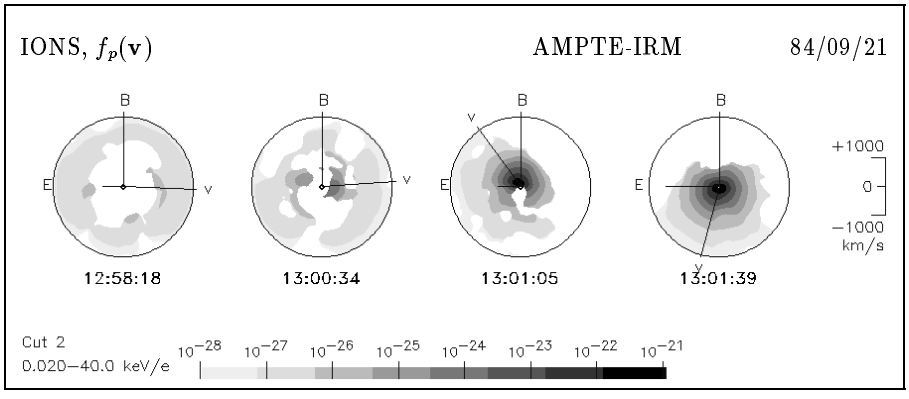

Fig. 3. Ion distributions in the energy range of 20 eV–40 keV measured on 21 September 1984. The format is the same as in Fig. 2.

No ion distribution and only one electron distribution was transmitted to the ground during the FTE. Similar to the electron distribution taken in the OBL, the distribution during the FTE shows solar wind electrons streaming parallel to **B**, which indicates that the field lines of the FTE are also connected to the northern hemisphere. It is consistent with the $+-$ signature of B_n during the FTE, if one assumes that an FTE is an encounter with an open magnetic flux tube and that the motion of the tube is dominated by the tension force that pulls the flux tube toward the hemisphere to which it is connected (e.g. Cowley, 1982). In Sect. 6, we will return to FTEs.

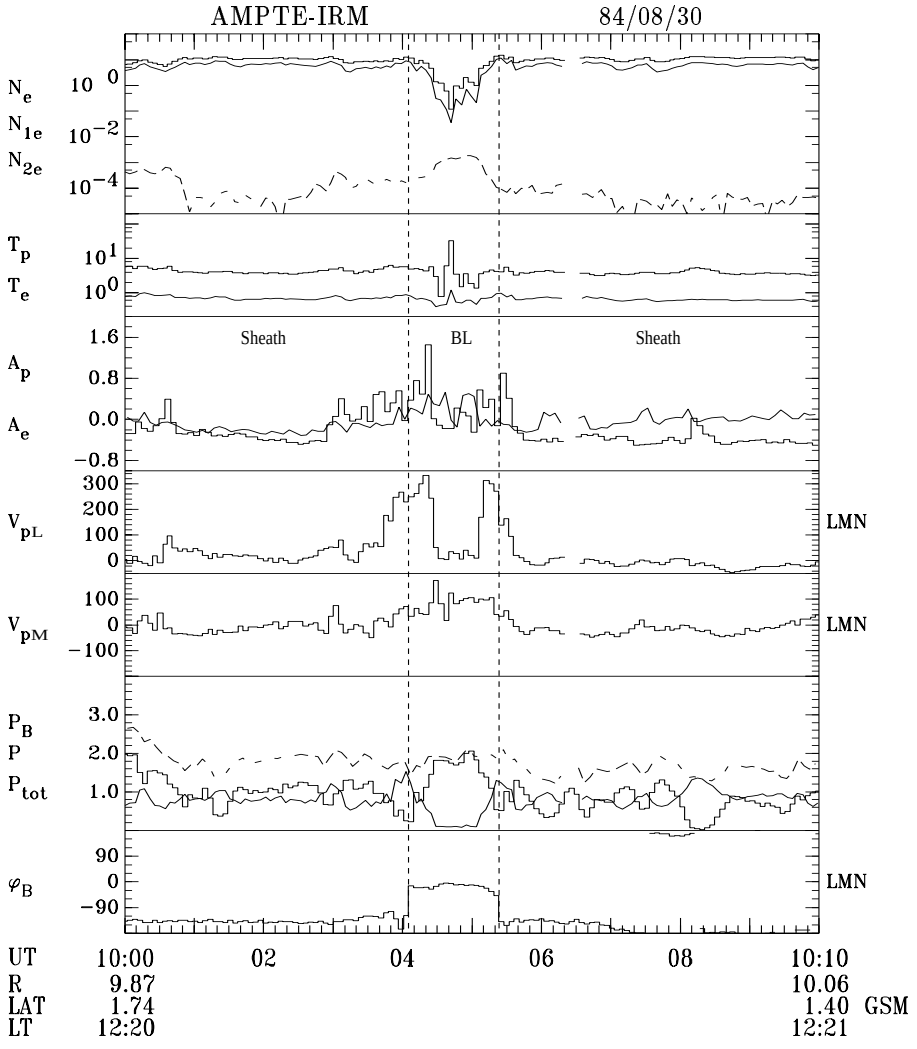

Fig. 4. Overview of the magnetopause pass on 30 August 1984. The format is the same as in Fig. 1.

3.2 Crossings on 30 August 1984

Figure 4, as well as panels a and b of Fig. 5 present a close pair of magnetopause crossings on 30 August 1984 at 2° northern GSM latitude at 12:20 LT. Both crossings can be identified as a sudden change in the angle φ_B by more than 90°. The inbound crossing occurs at 10:04:05 UT and the outbound crossing at 10:05:23. Between the two crossings, the IRM encounters the boundary layer. For this event, it is not possible to distinguish two separate parts of the boundary layer. While the electron distributions change gradually, the ion distributions are highly variable. Note the rather smooth transition of the total density N_e, and the partial densities N_{1e}, N_{2e} on the one hand, and the large variation of T_p and $A_p = T_{p\parallel}/T_{p\perp} - 1$ on the other hand. As we will see, the high values of A_p in the vicinity of the magnetopause are due to counterstreaming of different ion components.

In the panel of V_{pL}, we recognize, the northward directed reconnection flows. The existence of a de Hoffmann-Teller frame and the agreement with the Walén relation (2) was already tested for these flows by Paschmann et al. (1986) and Sonnerup et al. (1990). They found a good de Hoffmann-Teller frame and a fairly good correlation of the time series of $\mathbf{V}_p$ and $\mathbf{c}_A$. For the interval between 10:03:48–10:04:27 around the inbound crossing and for the interval between 10:05:06–10:05:45 around the outbound crossing, the de Hoffmann-Teller frame has $C_{E_c,E_{\rm HT}} = 0.89$, $\Lambda_{E_c,E_{\rm HT}} = 0.90$ and $C_{E_c,E_{\rm HT}} = 0.94$, $\Lambda_{E_c,E_{\rm HT}} = 0.96$, respectively. The cross-correlation C_{V,c_A} of the components along the maximum variance direction of **B** equals $+0.6$ and $+0.8$, respectively, indicating $B_n < 0$. The existence of a normal magnetic field B_n directed inward is confirmed by the electron distributions taken in the boundary layer at 10:04:16 and 10:04:46 (Fig. 5a), which show solar wind electrons streaming parallel to **B**, i.e. inward along open field lines. In the magnetosheath (10:02:10 and 10:04:03), the solar wind electrons exhibit a reduced flux along the spin axis which is due to an instrumental defect, described in Appendix 1 of Paschmann et al. (1986).

In Fig. 5b, we see a series of ion distributions measured in the magnetosheath well before the inbound crossing (10:02:49), in the magnetosheath close to the inbound

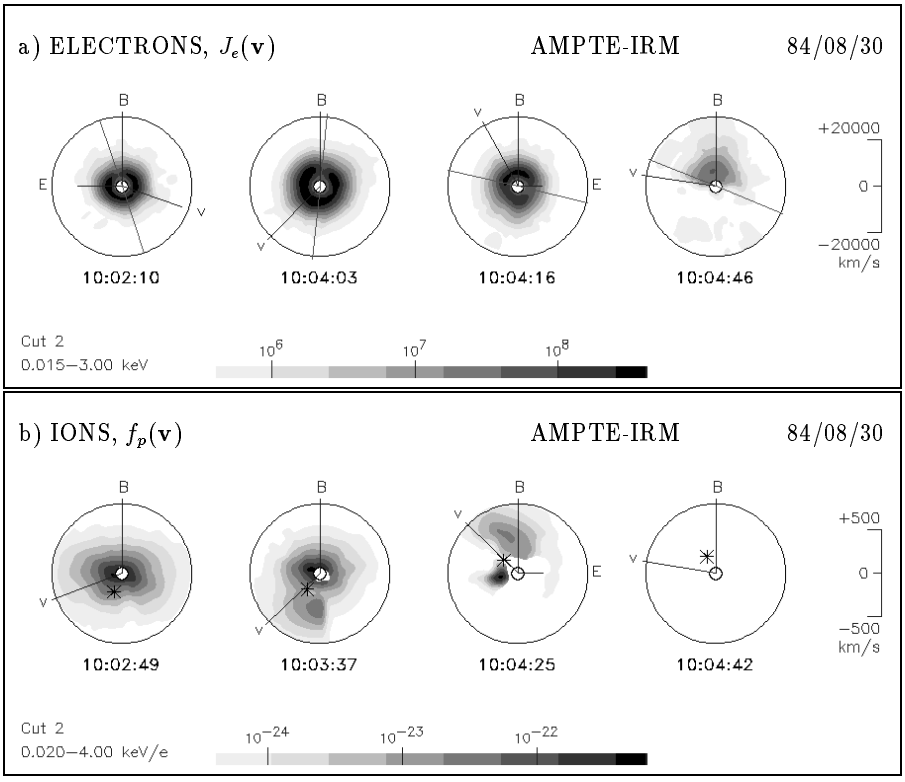

Fig. 5. Ion distributions in the energy range of 20 eV–4 keV and electron distributions in the range of 15 eV–3 keV measured on 30 August 1984. The format is the same as in Fig. 2.

magnetopause crossing (10:03:37), in the dense part of the boundary layer (10:04:25), and finally in its dilute part (10:04:42). The two magnetosheath distributions show an incident solar wind component flowing parallel to **B** with $V'_{i\parallel} \approx +0.6c_A$ in the de Hoffmann-Teller frame. Close to the magnetopause, reflected solar wind ions appear. As expected for reflection at a thin current layer, the field-aligned flow velocities in the de Hoffmann-Teller frame of the reflected ($V'_{r\parallel}$) and incident ($V'_{i\parallel}$) component fulfill $V'_{r\parallel} = -V'_{i\parallel}$, $V'_{i\parallel} > 0$ and $V'_{r\parallel} < 0$ which is consistent with $B_n < 0$, as deduced from the test of the Walén relation and the electron distributions in the boundary layer. The appearance of the reflected ions leads to the detected increase in A_p after ∼10:03.

In the boundary layer at 10:04:25, we recognize a maximum of the proton temperature anisotropy, $A_p \approx 1.5$. As can be seen in Fig. 5b, this field-aligned anisotropy is also due to counterstreaming of two components: the solar wind ions that have been transmitted across the magnetopausewhich have $v'_\parallel > 0$, which is again consistent with $B_n < 0$ and much colder ions, presumably of ionospheric origin which have $v'_\parallel < 0$ and thus stream outward along open field lines with $B_n < 0$. Due to the presence of the ionospheric ions, the field-aligned bulk velocity $V'_{p\parallel}$ in the de Hoffmann-Teller frame is only $+0.05c_A$ in the boundary layer. As described in Paschmann et al. (1985), $\mathbf{V}_p$ was computed under the assumption that all the ions were protons. If the ionospheric component contained many heavy ions, the actual $V'_{p\parallel}$ might even be negative. Although $V'_{p\parallel}/c_A$ is significantly different from $+1$, the reflected ions in the magnetosheath, the counterstreaming ions in the boundary layer, and the electron distributions in the boundary layer provide evidence for open field lines. At 10:04:42, in the dilute part of the boundary layer, no ions are visible within the energy range of Fig. 5b. However, the IRM detects hot ring current ions with $KT \approx 5\,\mathrm{keV}$ at that time.

3.3 Crossing on 17 September 1984

Figure 6 presents an overview of the inbound magnetopause crossing on 17 September 1984, which occurs at the 22° southern GSM latitude at 14:10 LT. The magnetopause is crossed at 10:47:58 UT. The rotation of the magnetic field across the magnetopause is low ($|\Delta\varphi_B| \approx 15°$) and we can see a clear plasma depletion layer (Zwan and Wolf, 1976). In Fig. 6, the plasma pressure decreases before 10:47:58 and the magnetic pressure increases. Furthermore, the existence of a plasma depletion layer is reflected in the strong perpendicular anisotropy, $A_p \approx -0.8$, of the proton temperature in the magnetosheath adjacent to the magnetopause. Performing a statistical survey, Phan et al. (1994) found that all low shear crossings have a plasma depletion layer, consistent with the expectation that magnetic reconnection is absent or less efficient between magnetic fields that are nearly parallel. The low shear magnetopause crossing on 17 September 1984 was included in their data set and it was also studied by Paschmann et al. (1993). In this section, we will show that the absence of magnetic reconnection, as inferred from the existence of a plasma depletion layer, is confirmed by tests

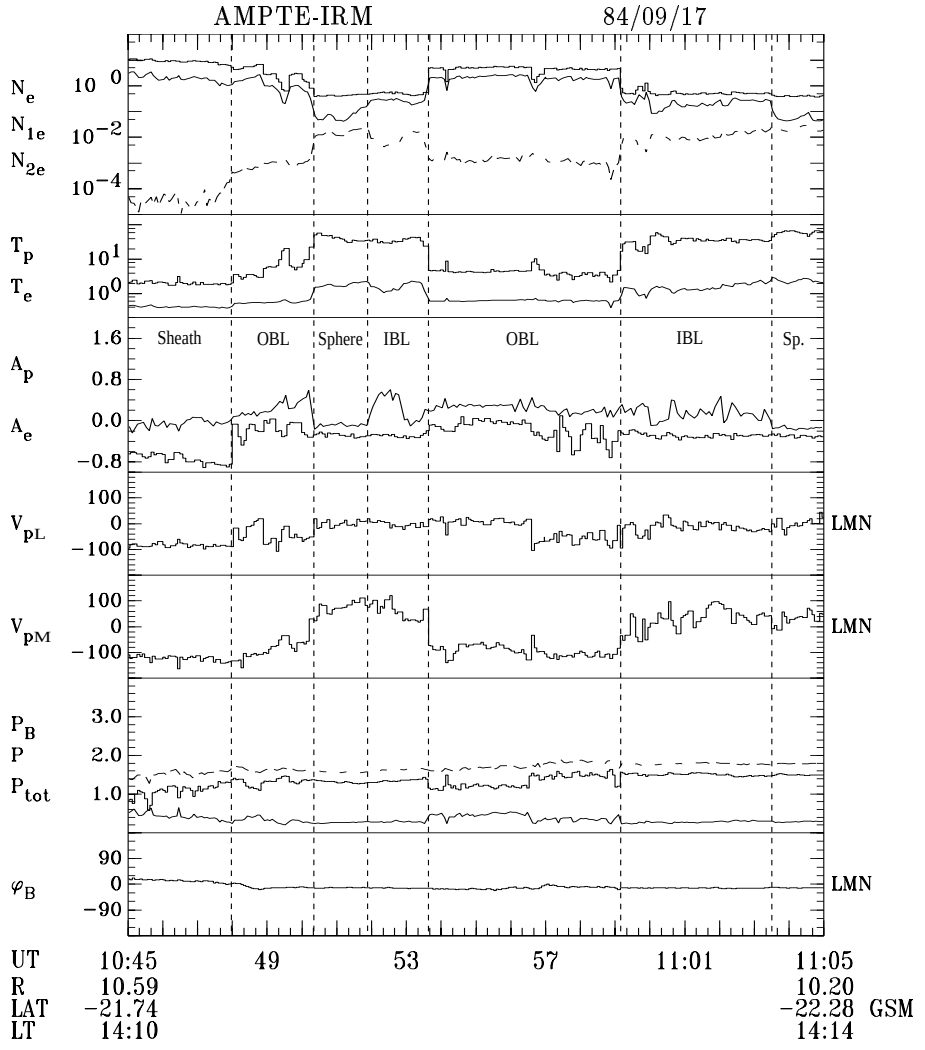

Fig. 6. Overview of the magnetopause pass on 17 September 1984. The format is the same as in Fig. 1.

for the prediction of a rotational discontinuity which will reveal that the local magnetopause is closed.

Since $|\Delta\varphi_B|$ is small, it is not possible to identify the magnetopause with the magnetic field data. But it is clearly visible in the plasma moments (Paschmann et al., 1993). Most striking is the sharp increase in A_p from its low value of about -0.8 in the plasma depletion layer to values of almost 0 after 10:47:58.

Similar to the high shear crossing on 21 September 1984, three different regions can be distinguished earthward of the magnetopause. From 10:47:58 to ∼10:50:20 and from 10:53:35 to 10:59:09, the IRM encounters the dense plasma of the OBL. Between ∼10:50:20 and ∼10:51:50 and after ∼11:03:30, IRM is located in the magnetosphere proper. An IBL with properties similar to those of the IBL observed on 21 September 1984 is encountered from ∼10:51:50 to 10:53:35 and from 10:59:09 to ∼11:03:30. In Fig. 6, the difference between the IBL and the magnetosphere is visible in the traces of N_{1e} and $A_e = T_{e\parallel}/T_{e\perp} - 1$. It is not possible to find a de Hoffmann-Teller frame for the interval between 10:47:27–10:48:37 around the magnetopause ($C_{E_c,E_{\rm HT}} = 0.57$, $\Lambda_{E_c,E_{\rm HT}} = 1.51$). Moreover, the time series of $\mathbf{V}_p$ and $\mathbf{c}_A$ are not correlated with one another, confirming that the local magnetopause is closed.

Figure 7b presents a series of ion distribution functions measured on 17 September 1984 in the magnetosheath (10:47:07), the OBL (10:54:10), the IBL (11:02:01), and the magnetosphere (11:04:55). We recognize that the solar wind population has a strong perpendicular anisotropy in the plasma depletion layer and is more isotropic in the OBL. A few solar wind ions are also detected in the IBL: note the narrow gray patch at $v \approx 200\,\mathrm{km/s}$ in the distribution taken at 11:02:01. Furthermore, hot ring current ions are observed in the IBL and magnetosphere proper. Having $KT \approx 10\,\mathrm{keV}$, they lie outside the energy range selected for Fig. 7b. None of the ion distributions show particle signatures predicted for open field lines.

Figure 7a presents electron distribution functions measured in the four regions. At 10:46:45 in the magnetosheath, the IRM detects solar wind electrons with $KT \approx 30\,\mathrm{eV}$. Across the magnetopause the field-aligned temperature of the solar wind electrons increases by a factor of 2, while their

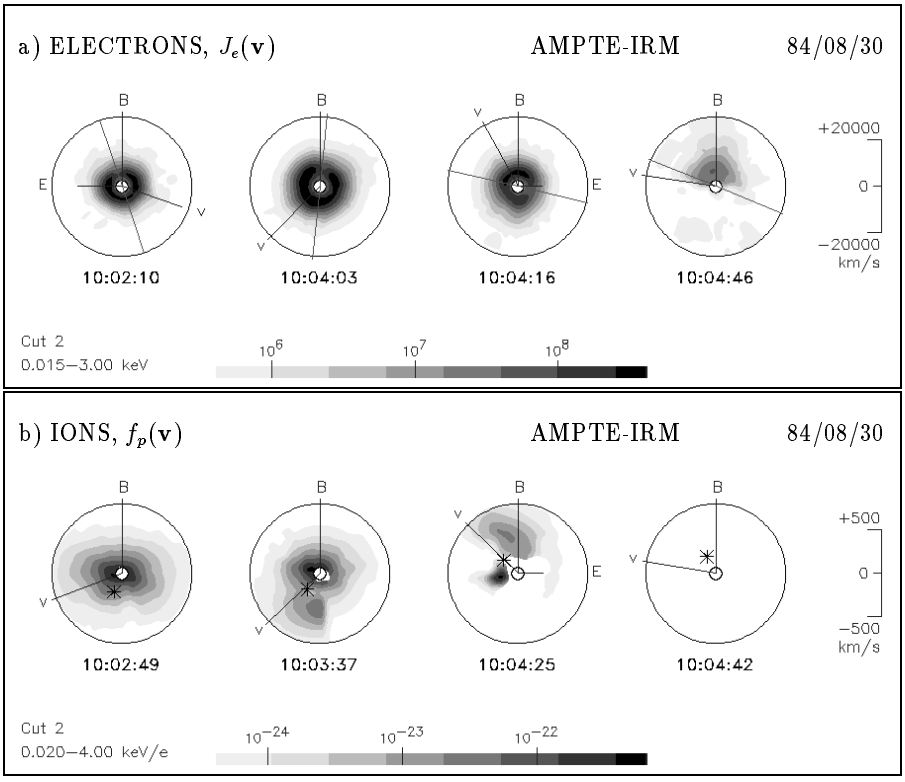

Fig. 7. Ion distributions in the energy range of 20 eV–4 keV and electron distributions in the range of 15 eV–3 keV measured on 17 September 1984. The format is the same as in Fig. 2.

perpendicular temperature increases only slightly. Unlike the distribution taken in the OBL on 21 September 1984, the electron distributions observed in the OBL on 17 September 1984, e.g. at 10:53:53, do not show any evidence for open magnetic field lines. The distributions taken in the IBL (11:02:23) and magnetosphere proper (11:04:38) are similar to those observed on 21 September 1984. In the magnetosphere proper, we find cold ($KT \sim 10\,\mathrm{eV}$) electrons presumably of ionospheric origin at velocities $v < 4000\,\mathrm{km/s}$ and hot ($KT \approx 1\,\mathrm{keV}$) ring current electrons at velocities $v > 10\,000\,\mathrm{km/s}$. Outside the energy range shown in Fig. 7a, a second ring current component with thermal energy $KT \sim 10\,\mathrm{keV}$ is detected. Both ring current components show the perpendicular temperature anisotropy characteristic of particles trapped in the geomagnetic field. In the IBL, e.g. at 11:02:23, we recognize again warm electrons at field-aligned velocities $v_\parallel \approx 8000\,\mathrm{km/s}$.

Similar to the crossing on 21 September 1984, important information about the IBL, can be deduced from the time series of N_{2e} and V_{pM}. In the IBL the partial density N_{2e} of electrons above 1.8 keV is again comparable to N_{2e} in the magnetosphere proper, but it drops in the OBL. Of course, this drop is also visible in Fig. 7a. The trace of V_{pM} indicates again a flow reversal at the interface between the OBL and the IBL. Since the IRM is located at 14:00 LT, the magnetosheath flow has a duskward component, $V_{pM} \approx -100\,\mathrm{km/s}$. While the flow in the OBL shares this duskward motion, the flow in the IBL and magnetosphere proper is directed dawnward. This reveals that the plasma in the IBL is not magnetically or viscously coupled to the magnetosheath plasma. Rather, the dawnward motion is consistent with the return flow of a closed magnetic flux from the nightside back to the dayside.

While the time series of N_{2e} and V_{pM} provide evidence that the IBL is on closed field lines, it is difficult to decide on the state of the OBL. On the one hand, the existence of a plasma depletion layer and tests for the prediction of a rotational discontinuity imply that the magnetopause is locally closed. On the other hand, cross-field diffusion should not be able to form an OBL whose density and temperature profiles show a plateau (10:53:35–10:59:09) with a sharp step at its inner edge. A possible explanation for the OBL on 17 September 1984 would be that it is on open field lines that cross the magnetopause at a location farther away from the spacecraft. In this case, the solar wind plasma detected in the OBL may have entered along open field lines. If these field lines do not cross the magnetopause locally but farther away from the spacecraft, there is no reason why the observed local magnetopause should have the properties of a rotational discontinuity.

3.4 Crossing on 84/11/30

Figure 8 presents an overview of the inbound magnetopause crossing on 30 November 1984, which occurs at the 3° northern GSM latitude at 10:30 LT. We identify the magnetopause as the increase in the proton temperature, the electron temperature, and the temperature anisotropies, A_p and

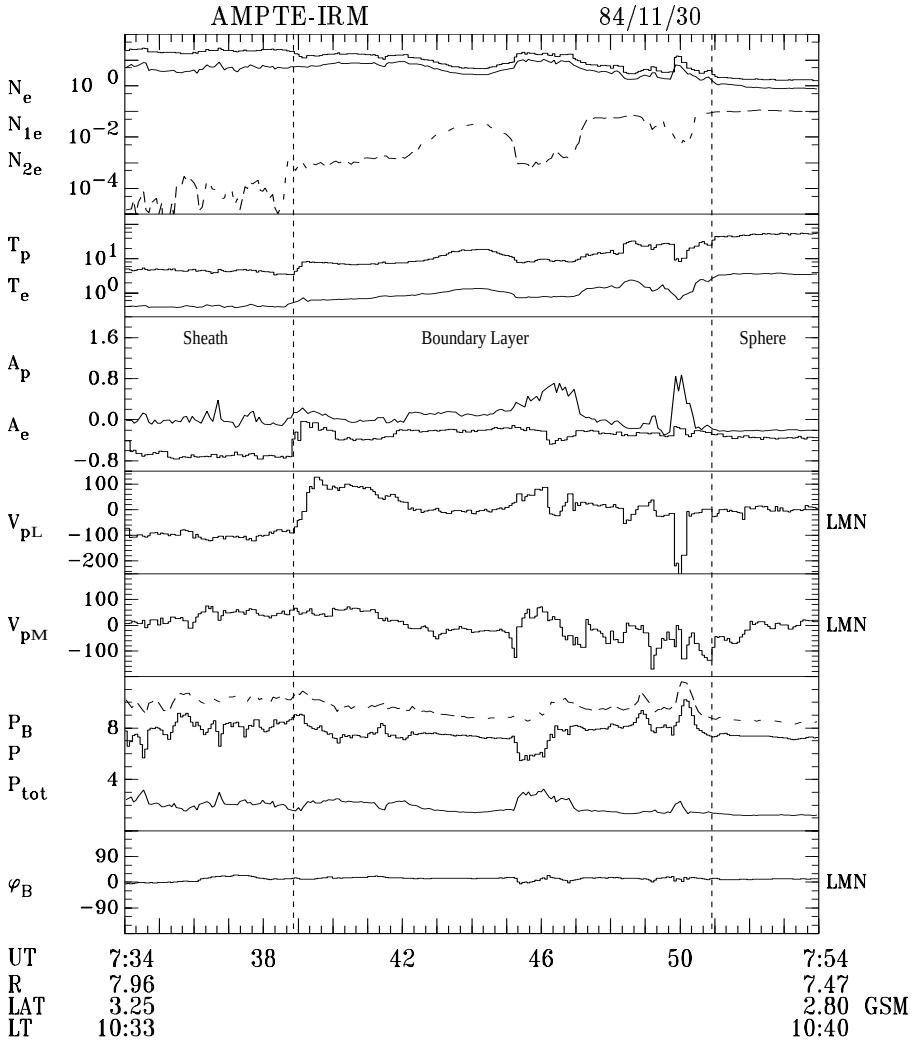

Fig. 8. Overview of the magnetopause pass on 30 November 1984. The format is the same as in Fig. 1.

A_e, at 07:38:51. The panel of φ_B shows that the direction of the tangential magnetic field does not change across the magnetopause. Immediately earthward of the magnetopause the component V_{pL} of the proton bulk velocity changes by about 200 km/s. Since this change of the tangential velocity is not accompanied by any change of the tangential magnetic field, the Walén relation (2) cannot be satisfied. Since in the interval 07:37:52–07:39:50 around the magnetopause $C_{E_c,E_{\rm HT}} = 0.59$, $\Lambda_{E_c,E_{\rm HT}} = 2.86$, we conclude that a de Hoffmann-Teller frame is improbable during this interval at least when it is based on our analysis.

The boundary layer lasts from 07:38:51 to ∼07:50:55. During this interval, the density oscillates a few times between about $20\,{\rm cm}^{-3}$ and $2\,{\rm cm}^{-3}$. The temperatures T_p and T_e exhibit similar oscillations. Since the temporal profiles of these oscillations are gradual rather than in steps, we do not distinguish between the OBL and the IBL.

Panel a of Fig. 9 presents a series of electron distributions measured on 30 November 1984 in the magnetosheath (07:38:20), the magnetosheath closer to the magnetopause (07:38:42), the boundary layer (07:40:05), and the magnetosphere proper (07:52:38). Panel b shows the ion distribution functions measured at the same times. In the magnetosphere, the IRM detects hot ring current ions with $KT \approx 6\,{\rm keV}$ and ring current electrons with $KT \approx 0.5\,{\rm keV}$. Both species show the perpendicular temperature anisotropy of trapped particles.

The electron distribution taken at 07:38:20 in the magnetosheath shows solar wind electrons with thermal energy $KT \approx 30\,{\rm eV}$. Closer to the magnetopause (07:38:42), the electron distribution becomes skewed along the magnetic field: it remains unchanged for $v_\parallel < 0$, whereas the other half of the distribution ($v_\parallel > 0$) is much flatter than at 07:38:20 and thus extends to higher energies. Skewed distributions such as the one taken at 07:38:42 were already reported by Fuselier et al. (1995) and interpreted as a feature of the magnetosheath boundary layer, i.e. the portion of the magnetosheath on reconnected field lines. According to this model, the electron distribution at 07:38:42 would indicate magnetic connection to the southern hemisphere ($B_n > 0$). Since $B_n > 0$ electrons with $v_\parallel < 0$ come from the solar wind end of an open field line, the half of the distribu-

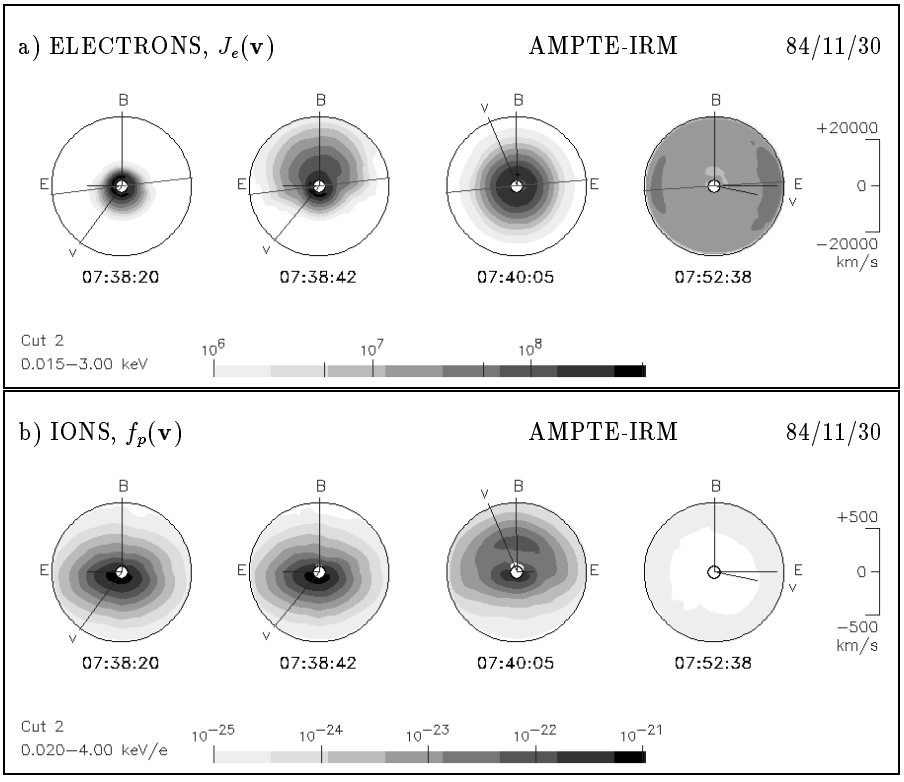

Fig. 9. Ion distributions in the energy range of 20 eV–4 keV and electron distributions in the range of 15 eV–3 keV measured on 30 November 1984. The format is the same as in Fig. 2.

tion antiparallel to **B** looks the same in the magnetosheath boundary layer as wellas in the magnetosheath on interplanetary field lines which are not yet reconnected. Electrons in the magnetosheath boundary layer with $v_\parallel > 0$ come from the terrestrial end of an open field line; the half of the distribution parallel to **B** should look similar to the low-latitude boundary layer earthward of the magnetopause. The electron plasma observed in the boundary layer at 07:40:05 has indeed a higher temperature than that in the magnetosheath, which could explain why the half of the distribution parallel to **B** at 07:38:42 is flatter than the half of the distribution antiparallel to **B**. In the model of Fuselier et al. (1995), solar wind electrons are heated when they cross the open magnetopause antiparallel to **B** from the magnetosheath to the boundary layer. After mirroring at low altitudes, they cross the open magnetopause again from the boundary layer to the magnetosheath and can be observed in the magnetosheath boundary layer, now moving parallel to **B**. The reason for the electron heating across the magnetopause is not known, but it is well established by observations (e.g. Paschmann et al., 1993) that the solar wind population in the boundary layer is primarily hotter than in the magnetosheath (see also Fig. 7a).

The half of the distribution parallel to **B** at 07:38:42 is even flatter than the distribution in the low-latitude boundary layer. One might speculate that this is the case due to the outward moving electrons in the magnetosheath boundary layer crossing the magnetopause twice and, therefore, heating twice. The heating of solar wind electrons is of course only one reason for the increase in T_e across the magnetopause. The other reason is the admixture of hot ring current electrons. For $v > 20\,000\,\mathrm{km/s}$, the phase space density in the magnetosphere proper is clearly higher than in the boundary layer and magnetosheath. Therefore, electrons with $v > 20\,000\,\mathrm{km/s}$ at 07:38:42 are probably ring current electrons leaking out to the magnetosheath.

Let us return to the ion distributions. At 07:38:20 and 07:38:42, the IRM detects the solar wind population of the magnetosheath. At 07:40:05 in the boundary layer, we see two components, i.e. two peaks of $f_p(\mathbf{v})$. One component appears at the same position in velocity space as the solar wind population in the magnetosheath. Thus, this component probably consists of solar wind ions that have entered the boundary layer locally due to diffusion or reconnection. The second component has a high field-aligned flow velocity, $V_\parallel \approx 350\,\mathrm{km/s}$, which suggests that it has entered the boundary layer at a location south of the spacecraft. At that location, either the flow velocity in the magnetosheath was different from the flow velocity observed in the local magnetosheath, or the acceleration across the magnetopause was different. The appearance of this second component is responsible for the change in V_{pL} around 07:39. Both components are observed throughout the boundary layer. There are several many IRM magnetopause passes that show ion distributions in the boundary layer with two solar wind components.

Table 1. Occurrence rate of reconnection signatures for high and low magnetic shear

	high shear	low shear
Walén event	42%	19%
at least one particle signature	75%	38%
bipolar B_n signature	46%	0%

4 Data set for statistical survey

We studied all IRM passes through the dayside (08:00–16:00 LT) magnetopause region for which magnetometer measurements, plasma moments at spin resolution, ion and electron distribution functions of the full energy-per-charge range, and electric wave spectra are available. The statistical data set, analyzed in this paper and in paper 2, contains all magnetopause crossings that occurred during these passes and that fulfill the following selection criteria: (1) The crossing is a complete crossing from the magnetosheath to the magnetosphere proper (or vice versa). (2) The boundary layer lasts for $\Delta t_{\rm BL} > 30$ s. (3) At least two electron distribution functions are measured in the boundary layer. (4) The time intervals in the magnetosheath before (after) the boundary layer and the time interval in the magnetosphere after (before) the boundary layer are sufficiently long so that an unambiguous identification of the magnetopause and of the earthward edge of the boundary layer is possible.

Criteria 2 and 3 are required in order to resolve the internal structure of the boundary layer, i.e. to distinguish gradual time profiles from step like profiles. Due to criterion 2, our data set is likely to be biased toward crossings of thick boundary layers. Note, however, that Phan and Paschmann (1996) found a trend for crossings with long boundary layer duration to result from lower magnetopause speeds. Thus boundary layers lasting more than 30 s need not necessarily be much thicker than those of a shorter time duration.

With the above selection criteria, we obtained 40 magnetopause crossings. The magnetopause crossings on 17 September 1984 (Sect. 3.3), on 21 September 1984 (Sect. 3.1), and on 30 November 1984 (Sect. 3.4) are included in the statistical data set. However, the two crossings on 30 November 1984 (Sect. 3.2) are not included, since the IRM does not encounter the magnetosphere proper.

We will distinguish between low and high magnetic shear. Choosing 40° as the dividing line, we obtain 16 low shear ($|\Delta\varphi_B| < 40^\circ$) crossings and 24 high shear ($|\Delta\varphi_B| > 40^\circ$) crossings. All crossings occurred near the equatorial plane, at latitudes less than 30°. The numbers of crossings in the local time sectors 08:00–10:00, 10:00–12:00, 12:00–14:00, and 14:00–16:00 are 12, 14, 7, and 7, respectively.

5 Agreement with Walén relation

In this section, we test for the existence of a de Hoffmann-Teller frame and for the agreement with the Walén relation for the 40 magnetopause crossings in the statistical data set. The tests are performed for a time interval approximately centered at the magnetopause that is at least 20 s long, but may be much longer if the duration of the boundary layer is long.

First, an estimate of the de Hoffmann-Teller velocity, $\mathbf{V}_{\rm HT}$, is determined by minimizing the quadratic form D of Eq. (1). For a reasonable de Hoffmann-Teller frame, we require that the minimum of D is well-defined and that $\mathbf{V}_{\rm HT}$ is stable when the interval used for the test is varied. Then the fit between $\mathbf{E}_c = -\mathbf{V}_p \times \mathbf{B}$ and $\mathbf{E}_{\rm HT} = -\mathbf{V}_{\rm HT} \times \mathbf{B}$ is checked by producing a single scatter plot of $-\mathbf{V}_p \times \mathbf{B}$ versus $-\mathbf{V}_{\rm HT} \times \mathbf{B}$ (Sonnerup et al., 1987, 1990; Paschmann et al., 1990) and its correlation coefficient and linear regression coefficients are calculated. Moreover, we calculate the cross correlation and the linear regression coefficients of the time series of the components $-\mathbf{V}_p \times \mathbf{B}$ and $-\mathbf{V}_{\rm HT} \times \mathbf{B}$ along the maximum variance direction of $-\mathbf{V}_p \times \mathbf{B}$. Inspecting the scatter plots and the correlation and regression coefficients, we find that 26 of the 40 crossings have a reasonable de Hoffmann-Teller frame. For 10 of the 14 events without de Hoffmann-Teller frame, the magnetic shear across the magnetopause is low ($|\Delta\varphi_B| < 40^\circ$) and for 4 events, it is high ($|\Delta\varphi_B| > 40^\circ$).

The agreement with the Walén relation (2) is checked with the help of the scatter plot of $\mathbf{V}'_p = \mathbf{V}_p - \mathbf{V}_{\rm HT}$ versus $\mathbf{c}_A$ and by calculating the correlation and linear regression coefficients. We also calculate the cross correlation and linear regression coefficients of the time series of the components $\mathbf{V}'_p$ and $\mathbf{c}_A$ along the maximum variance direction of $\mathbf{B}$. We find that 13 of the 26 magnetopause crossings have a reasonable de Hoffmann-Teller frame and the relation

$$\mathbf{V}'_p = \Lambda \mathbf{c}_A \tag{3}$$

is approximately satisfied. For the remaining 13 crossings. $\mathbf{V}'_p$ and $\mathbf{c}_A$ are not correlated .

One of the 13 magnetopause crossings satisfying Eq. (3) agrees perfectly with the Walén relation ($|\Lambda| = 1$). For 2 crossings, $|\Lambda|$ is only 0.2. For the remaining 10 crossings, $|\Lambda|$ is in the range of 0.4–0.8. The fit between the prediction of the Walén relation and the measured plasma moments and magnetic fields was tested in numerous studies of magnetopause crossings (e.g. Paschmann et al., 1986, 1990; Sonnerup et al., 1987, 1990). As in our survey, it was found that a linear relation (3) existed for many crossings, but the magnitude of the slope Λ is primarily less than 1.

What can we infer from the linear relation (3)? First, Eq. (3) gives a qualitative indication of an open magnetopause. There is no reason to expect such a relation for a closed magnetopause. On the other hand, a magnetopause crossing that satisfies Eq. (3) with $|\Lambda| < 1$ does not agree quantitatively with the theory of the rotational discontinuity. We have noted reasons for the deviations in the Intro-

duction (see also Scudder, 1997). It cannot be expected that our analysis which is based on ion bulk flows will provide ideal agreement. But the existence of a satisfactory fit to the above equation can safely be taken as confirmation of an approximate validity of the model. The three magnetopause crossings studied in Sects. 3.1 and 3.2 provided us with additional information concerning the interpretation of Eq. (3). Although $|\Lambda|$ is significantly less than 1 for those crossings, the observed particle signatures in the distribution functions provide some evidence for open field lines. The sign of B_n inferred from the particle signatures is consistent with the sign of B_n inferred from Eq. (3).

In Sect. 7, we will investigate how often particle signatures expected on open field lines occur during the 40 crossings of the statistical data set. For particle signatures observed during the 13 magnetopause crossings showing a linear relation (3), the sign of B_n as inferred from the respective particle signature will be compared with the sign of B_n as inferred from Eq. (3). As we will see, there are observations of particle signatures for which the sign of B_n inferred from the particle signature differs from the sign of B_n inferred from Eq. (3). But for the clear majority of observations of particle signatures, the sign of B_n inferred from the particle signature coincides with the sign of B_n inferred from Eq. (3). For the types of particle signatures observed frequently, this coincidence shows that it is correct, in a statistical sense, to interpret the respective type of particle signature in terms of open field lines. Vice versa, it can also be concluded that it is correct, in a statistical sense, to consider the validity of Eq. (3) as an indication of an open magnetopause. Hence, we will from now on consider the validity of Eq. (3) as a "reasonable agreement with the Walén relation" and refer to the magnetopause crossings showing a linear relation (3) as "Walén events". The reasons why $|\Lambda|$ is, in general, less than 1 will be discussed in Sect. 8.

For 9 of the 13 Walén events, the sign of Λ is positive, which indicates $B_n < 0$ and for 4 events it is negative ($B_n > 0$). For 11 of the 13 Walén events, the boundary layer can be divided into an OBL and IBL, whereas 2 Walén events have a gradual density profile. Three of the 13 Walén events are low shear crossings and 10 are high shear crossings. The percentage of Walén events and non-Walén events for high and low magnetic shear across the magnetopause, respectively, is illustrated in Table 1.

In their survey of a set of IRM high shear crossings, Phan et al. (1996) checked the fit between the observed change $\Delta\mathbf{V}_p$ of the proton bulk velocity across the magnetopause and the change $\pm\Delta\mathbf{c}_A$ of the Alfvén velocity. $\Delta\mathbf{V}_p$ and $\Delta\mathbf{c}_A$ were both computed for each measurement in the boundary layer as the difference between the respective measurement in the boundary layer and the average of a reference interval in the magnetosheath. For each magnetopause crossing, the agreement with the prediction of Eq. (2) was then quantified by computing the index

$$\Delta V^* = \frac{\Delta\mathbf{V}_p \cdot \Delta\mathbf{c}_A}{|\Delta\mathbf{c}_A|^2} \tag{4}$$

Finally, a magnetopause crossing was considered to be in reasonable agreement with the Walén relation, if $|\Delta V^*|$ evaluated at the time of the maximum observed velocity change $\Delta\mathbf{V}_p$ was greater than 0.5. Using this criterion, which differs from ours, Phan et al. (1996) found that 61% of the high shear crossings are in reasonable agreement with the Walén relation, whereas our survey reveals that 42% of the high shear crossings are Walén events.

6 Flux transfer events

By looking for clear bipolar pulses in the time series of the normal magnetic field, B_n, we can identify magnetosheath FTEs during 5 of the 40 magnetopause crossings and magnetospheric FTEs during 9 of the 40 magnetopause crossings in our data set. During 3 crossings, both magnetosheath and magnetospheric FTEs are observed and during 8 crossings, only one type of FTEs is observed. For 3 of the 11 crossings with FTEs, the magnetic shear angle, $|\Delta\varphi_B|$, measured across the magnetopause is $50°$–$60°$. The remaining 8 crossings had shear angles of $90°$ or more. This is in line with the finding (e.g. Rijnbeek et al., 1984; Southwood et al., 1986) that FTEs are favored by a southward directed interplanetary magnetic field.

In the original FTE model of Russell and Elphic (1978), an FTE is an encounter with a reconnected magnetic flux tube. A flux tube moving northward causes a $+-$ bipolar signature of B_n, whereas a flux tube moving southward causes a $-+$ signature. If the motion of the flux tube is dominated by the magnetic tension force, a flux tube connected to the northern hemisphere ($B_n < 0$) moves northward and causes a $+-$ signature, whereas a flux tube connected to the southern hemisphere ($B_n > 0$) moves southward and causes a $-+$ signature. Assuming that the motion of the flux tube is dominated by the tension force, one can thus infer the sign of the normal magnetic field B_n in the reconnected flux tube from the orientation ($+-$ or $-+$) of the bipolar signature.

For the Walén events in our data set, we can compare the sign of B_n inferred from the bipolar signature of FTEs with the sign of B_n as inferred from Eq. (3). Magnetosheath FTEs are observed during 3 of the 13 Walén events and magnetospheric FTEs are observed during 5 of the 13 Walén events. We find that for all FTEs observed during Walén events, the sign of B_n inferred from the bipolar signature coincides with the sign of B_n inferred from Eq. (3). Thus, we can explain all FTEs observed during Walén events as encounters with reconnected flux tubes that are connected to the same hemisphere as the field lines in the vicinity of the magnetopause and that move toward the hemisphere to which they are connected. Our result can also be explained by other reconnection models of FTEs. In any case, it provides evidence for FTEs as a signature of magnetic merging.

Table 2. Occurrence rate of particle signatures and bipolar B_n signatures during Walén and non-Walén events. For the Walén events, it is given how often the signature is consistent with Eq. (3)

	Walén (consist.)	non-Walén
electron heat flux	62% (54%)	15%
escaping RC ions	31% (31%)	0%
D-shaped	23% (23%)	15%
counterstr. SW/cold	23% (15%)	19%
skewed SW distr.	62% (54%)	15%
at least one part. sign.	77%	52%
bipolar B_n signature	62% (62%)	19%

7 Occurrence of particle signatures

In Sect. 3 we reported on examples of observations of several types of single particle signatures expected on open magnetic field lines. Now we study the occurrence frequency of the various types of particle signatures. For Walén events, we compare the sign of B_n as inferred from the respective particle signature with the sign of B_n inferred from Eq. (3). If the number of Walén events, for which a particular type of particle signature is consistent with Eq. (3), is high compared to the number of Walén events for which it is not consistent, the respective type of signature can be considered as a reliable indicator of open field lines. If these two numbers are comparable, the respective signature may be caused by mechanisms other than reconnection. In Table 2 the occurrence rates are given as percentages.

7.1 Electron heat flux

In Sect. 3 we examined two kinds of electron distributions associated with substantial heat flux along the magnetic field. On 21 September 1984 at 13:01:05 (Fig. 2a), the heat flux is caused by hot ring current electrons escaping along **B** from the magnetosphere to the magnetosheath. On 30 November 1984 at 07:38:42 (Fig. 9a), part of the heat flux is due to a skewed distribution of solar wind electrons. Both the escape of ring current electrons and the skewed distribution of solar wind electrons (Fuselier et al., 1995) are expected to lead to heat flux that is directed outward from the magnetosphere to the magnetosheath. Thus, heat flux antiparallel to **B** indicates $B_n < 0$ and heat flux parallel to **B** indicates $B_n > 0$. How often do we observe substantial electron heat flux at the magnetopause?

In Sects. 7.1 to 7.5 we study the occurrence frequency of various types of particle signatures by counting the magnetopause crossings in the data set during which the respective type of signature is observed. When we count the crossings, we take only crossings for which the particular type of particle signature fulfills the following criteria: (1) The particle signature is clearly visible when the measured distribution functions are inspected by eye. (2) The orientation of the particle signature (parallel or antiparallel to **B**) does not change during the crossing.

In the case of electron heat flux, e.g. criteria 1 and 2 imply that we do not consider the weak heat flux that is practically always observed due to the limited accuracy of the instrument or due to the variations in the real electron distribution within a spin period of IRM. Furthermore, criterion 2 sorts out magnetopause crossings for which the electron heat flux is strong, but changes its orientation in the course of the crossing from parallel to **B** to antiparallel to **B** or vice versa. Such observations might indicate time dependent patchy reconnection or encounters with the vicinity of the X-line. However, they cannot be used to infer the sign of B_n from the orientation of the electron heat flux or to check whether this sign is consistent with Eq. (3). The implications of criteria 1 and 2 for the other particle signatures of Sects. 7.2 to 7.5 are analogous.

Applying criteria 1 and 2, we count the magnetopause crossings with electron heat flux. Thereby, we do not distinguish whether the heat flux is due to a streaming of ring current electrons or due to a field-aligned, skewed distribution of solar wind electrons. We find that electron heat flux is observed during 12 of the 40 magnetopause crossings in the data set. Of those 12 crossings, 8 are Walén events. For one Walén event the orientation of the electron heat flux is inconsistent with the sign of B_n inferred from Eq. (3), but it is consistent for the other 7 Walén events. Hence, electron heat flux fulfilling criteria 1 and 2 is primarily consistent with Eq. (3) and can, in a statistical sense, be considered as a useful indicator of open field lines.

7.2 Escape of ring current ions

On 21 September 1984 at 13:01:39 (Fig. 3), we observe hot ring current ions escaping from the magnetosphere to the magnetosheath. This escape along open field lines is associated with a substantial outward directed proton heat flux, $H_{p\parallel} \approx -0.05\,\mathrm{mW/m^2}$. Inspecting all ion distribution functions measured during the crossings of the statistical data set, we find a streaming of ring current ions for 4 out of the 40 crossings. These 4 magnetopause crossings are all Walén events and the orientation of the outward directed heat flux is consistent with the sign of B_n inferred from Eq. (3).

7.3 "D-shaped" distributions of solar wind particles

On 21 September 1984 at 13:01:05 (Fig. 2), we observe "D-shaped" distributions of solar wind ions and electrons. When we search for "D-shaped" distributions of solar wind particles in the statistical data set, we require that the measured phase space density is cut off at $v'_{\parallel} \approx 0$, as observed on 21 September 1984 at 13:01:05. We find that "D-shaped" distributions of solar wind electrons are measured during 2 of the 40 crossings. On 21 September 1984 the orientation of the "D" is consistent with the sign of B_n inferred from Eq. (3). The other crossing is not a Walén event. "D-shaped" distributions of solar wind ions are measured during 5 of the 40

crossings. For all 5 crossings, the magnetic shear across the magnetopause is high. Of the 5 crossings, 2 are Walén events and for these 2 crossings, the orientation of the "D" is consistent with the sign of B_n inferred from Eq. (3).

7.4 Counterstreaming of solar wind ions and cold ions

On 30 August 1984 at 10:04:25 (Fig. 5b), we observe solar wind ions streaming inward along open field lines and cold ions, presumably of ionospheric origin, simultaneously streaming outward. By looking for the counterstreaming of solar wind and cold ions in the entire data set, we find this signature for 8 out of 40 crossings. Three of these 8 crossings are Walén events. If the counterstreaming is due to magnetic reconnection, it can be used to infer the sign of the normal magnetic field B_n: streaming of the solar wind ions relative to the cold ions parallel (antiparallel) to **B** indicates $B_n < 0$ ($B_n > 0$). For 2 of the 3 Walén events, the sign of B_n inferred from the counterstreaming agrees with the sign of B_n inferred from Eq. (3).

The crossing where the counterstreaming of solar wind and cold ions is inconsistent with Eq. (3) occurred on 30 August 1984 at 09:56:43, roughly 8 min before the two crossings studied in Sect. 3.2. Remember that those two crossings are not included in our data set, because the magnetosphere proper is not encountered. Similar to the other two crossings, the test of the Walén relation indicates $B_n < 0$ for the magnetopause crossing at 09:56:43. Immediately earthward of the magnetopause, the flow velocity of the transmitted solar wind component in the de Hoffmann-Teller frame is about 200 km/s. At 09:51:54, when the counterstreaming of solar wind and cold ions is observed, the flow velocity of the solar wind component in the de Hoffmann-Teller frame is about $-500\,\mathrm{km/s}$. Thus, the solar wind component at 09:51:54 cannot be identical to the transmitted component observed immediately earthward of the magnetopause. The field lines encountered at 09:51:54 are probably topologically different from those encountered immediately earthward of the magnetopause.

7.5 Skewed distributions of solar wind ions

What do we mean by skewed distributions? Two examples of skewed distributions of solar wind ions are those measured on 30 August 1984 at 10:03:37 (Fig. 5b) and on 30 November 1984 at 07:40:05 (Fig. 9b). Both distributions show two beams, i.e. two peaks of $f_p(\mathbf{v})$. The reflected solar wind ions detected on 30 August 1984 at 10:03:37 in the magnetosheath close to the magnetopause lead to a field-aligned heat flux, $H_{p\|} \approx -0.14\,\mathrm{mW/m^2}$. In the magnetosheath we furthermore observe ion distribution functions that are also associated with a substantial field-aligned heat flux, but do not show two peaks of $f_p(\mathbf{v})$. Rather these distributions consist of a steep, half parallel to **B**, and a flat, half antiparallel to **B** or vice versa. By examining both of these "steep-flat" distributions and the two-beam distributions observed in the magnetosheath for Walén events, we find that the proton heat flux associated with these distributions is, in most cases, outward along open field lines.

"Steep-flat" distributions are also observed in the boundary layer, the heat flux associated with "steep-flat" distributions measured during Walén events is directed outward along open field lines in most cases, as well. The distribution taken on 30 Nobember 1984 at 07:40:05 is an example of a two-beam distribution measured in the boundary layer. It is associated with a substantial proton heat flux, $H_{p\|} \approx 0.08\,\mathrm{mW/m^2}$.

Why do we observe two beams in the boundary layer? One possibility is that beam 1 consists of locally entering ions and beam 2 consists of ions that have entered the boundary layer at a remote location. This interpretation was given for the distribution measured on 30 November 1984 at 07:40:05. Similar two-beam distributions have been presented by Nakamura et al. (1997). Another possibility is that beam 2 is produced when beam 1 is mirrored at low altitudes. In this case, the field-aligned components of the flow velocities of the two beams should have about the same magnitude, but opposite sign in the spacecraft frame. Two-beam distributions fulfilling this condition were reported by Onsager and Fuselier (1994) and are also seen in the IRM data.

Can we use skewed distributions of solar wind ions to infer the sign of the normal magnetic field B_n? In the following, we try to infer B_n for three types of skewed distributions: (1) If we observe distributions of solar wind ions in the magnetosheath associated with a field-aligned heat flux, we assume that the heat flux is directed outward. (2) If we observe "steep-flat" distributions in the boundary layer, we assume that the heat flux is directed outward. (3) If we observe two-beam distributions in the boundary layer and are able to identify beam 1 as the component of locally entering solar wind ions, we assume that the field-aligned velocity of beam 2 relative to beam 1 is directed outward.

We find distribution functions of types 1–3 for 12 of the 40 magnetopause crossings in the data set. Eight of these 12 crossings are Walén events. By comparing the sign of B_n inferred from Eq. (3) with the sign of B_n inferred from the skewed distributions with the above assumptions, we find that those two methods of inferring the sign of B_n lead to the same result for 7 of the 8 Walén events. Hence, skewed distributions of solar wind ions can, in a statistical sense, be considered as a useful indicator of open field lines.

7.6 Events with at least one type of signature

So far, we counted the number of crossings showing a particular type of particle signature. Let us, in addition, count the number of magnetopause crossings that show at least one of the types of particle signatures studied in Sects. 7.1 to 7.5. We find that the particle signatures are more frequent for high shear (18 out of 24 crossings) than for low shear (6 out of 16). During 10 of the 13 Walén events, at least one particle signature of open field lines is observed. The corresponding percentages are given in Tables 1 and 2.

8 Discussion

By checking the fit between the IRM data and the prediction of the Walén relation (2), we found in Sect. 5 that a linear relation (3) is fulfilled for 13 (33%) of the magnetopause crossings in the statistical data set. By comparing the sign of the normal magnetic field B_n inferred from Eq. (3) with the sign of B_n inferred from particle signatures in the distribution functions, we found that the two methods of inferring B_n lead primarily to the same result. Thus, we conclude that the validity of Eq. (3) is a reliable indicator of an open magnetopause and that the local magnetopause is open approximately one-third of the time. Vice versa, it can be concluded that the sign of B_n inferred from the various particle signatures is primarily correct. In Sects. 7.1 to 7.5, we investigated the occurrence frequency of several types of particle signatures by counting the number of magnetopause crossings in the data set for which the respective type of signature is observed. None of the numbers that we obtained was greater than 12 (30%). On the other hand, 24 (60%) of the 40 crossings in the data set showed at least one of the types of particle signatures (Sect. 7.6). This may indicate that the plasma in the vicinity of the magnetopause is on open field lines considerably more often than one-third of the time. This discussion is based on the assumption of proton moments. In the current carrying the rotational discontinuity boundary layer, the direction of these fluxes may deviate from that of the electrons. This is a good reason for the above discrepancy. The approximate satisfaction of Eq. (3) can, therefore, under these conditions be taken as an argument in favor of the rotational discontinuity concept.

We consider the validity of Eq. (3) as a reasonable agreement with the Walén relation (2) and thus, an indicator for the open magnetopause. We discuss the question of why the magnitude of the field-aligned velocity in the de Hoffmann-Teller frame, $|V'_{p\|}|$, is less than the simultaneously measured Alfvén speed, c_A, for most Walén events. We use the crossings on 21 September 1984 (Sect. 3.1) and on 30 August 1984 (Sect. 3.2). For these crossings, the observed particle signatures alone provide evidence that the local magnetopause is open. One reason for $|V'_{p\|}/c_A| < 1$ may be the presence of heavy ions, which reduce the actual c_A to less than the computed c_A. Moreover, the rotational discontinuity is not well separated from the slow mode structure that Levy et al. (1964) located earthward of the rotational discontinuity. The slow mode is associated with an increase in c_A in the boundary layer. On 30 August 1984, c_A has indeed increased by a factor of 2, between 10:03:37 and 10:04:25. Correcting for this factor of 2 the value of $|V'_{p\|}/c_A|$ at 10:04:25 becomes 0.1. The measurement in the boundary layer on 21 September 1984 at 13:01:05 is taken sheathward of the increase in c_A.

Other reasons for $|V'_{p\|}/c_A| < 1$ are gradients in the plasma pressure tangential to the magnetopause. In a plasma with curved field lines, the force associated with plasma pressure gradients tends to oppose the tension force due to the field line curvature. At an open magnetopause tangential gradients of the pressure will act to reduce acceleration by magnetic tensions. Sonnerup et al. (1987, 1990) demonstrated that there are crossings for which the fit to the Walén relation can be considerably improved by introducing acceleration of the de Hoffmann-Teller frame.

It is once more important to note that Eq. (2) becomes inaccurate in the presence of electric currents. Scudder et al. (1999) and Puhl-Quinn and Scudder (2000) studied rotational discontinuities and Alfvén wave trains by performing a generalized Walén test on Polar data. This test was done by fitting a linear vector difference equation to the observed changes in electron bulk velocity, $\mathbf{V}_e$, and the magnetic field. The constant of proportionality determined from that fit could be compared with the theoretical prediction. For almost all cases where electron data agreed with the theoretical prediction, the corresponding fit to the ion data gave a constant of proportionality that was smaller in magnitude than implied by Eq. (2). This constant of proportionality is closely related to the slope Λ in Eq. (3) and the ratio $V'_{p\|}/c_A$. Thus, the low values of $|V'_{p\|}/c_A|$ may be due to our use of ion data collected in regions with electric currents.

A value $|V'_{p\|}/c_A| < 1$ is not the only discrepancy between the theory of a time stationary open magnetopause and the observations. In addition, there is also a considerable discrepancy between the particle distribution functions predicted for open field lines and those measured during the Walén events. Let us give two examples: according to Cowley (1982), the distributions of solar wind particles detected in the boundary layer should be "D shaped". However, we observe "D-shaped" distributions of solar wind particles only for the minority of the Walén events (Sect. 7.3). A possible explanation for this discrepancy is that the solar wind particles are mirrored at low altitudes and that the velocity cutoff disappears when the mirrored particles return to the magnetopause. This explanation may work for the electrons. However, for the ions, the time that passes until the mirrored ions return to the magnetopause is so long (~ 10 min) that "D-shaped" distributions of solar wind ions should be observed more frequently.

A similar discrepancy between predicted and observed distribution functions exists for hot ring current electrons, which, when electrons detected on reconnected field lines, should also have a "D shape" and stream outward. Such streaming is indeed observed for some of the Walén events (e.g. on 21 September 1984 at 13:01:05), but for most Walén events, ring current electrons observed in the boundary layer and magnetosheath close to the magnetopause do not show field-aligned streaming.

Is the local magnetopause closed for all non-Walén events? This need not be the case. The Walén relation cannot be satisfied near the X-line. If reconnection is time dependent and patchy, there are X-lines everywhere separating patches with $B_n < 0$ from patches with $B_n > 0$. In Sect. 7.1, it was mentioned that there are several magnetopause crossings for which a particular particle signature, e.g. the electron heat flux, changes its orientation in the course of the crossing from parallel to **B** to antiparallel to **B** or vice versa. This pro-

vides evidence that reconnection is indeed time dependent and patchy.

For several magnetopause crossings, e.g. the one on 17 September 1984, there is evidence that the local magnetopause was closed. But even for these cases, it is possible that part of the boundary layer is formed by reconnection. The field lines in the boundary layer may be open field lines crossing the magnetopause at a location farther away from the spacecraft or they may be field lines that have been first opened by reconnection, then filled with solar wind plasma, and reclosed later on. In paper 2 we will address the question of the formation of the low-latitude boundary layer in more detail.

Acknowledgement. We thank H. Lühr for making available the magnetic field data. We note with sadness the death of our selfless and skilled colleague Norbert Sckopke. We also thank the two referees for their criticisms and very helpful remarks on this lengthy and complicated investigation.

Topical Editor G. Chanteur thanks J. Scudder and M. Nakamura for their help in evaluating this paper.

References

Bauer, T. M., Treumann, R. A., and Baumjohann, W., The outer and inner low-latitude boundary layer, Ann. Geophysicæ, submitted, 2000.

Baumjohann, W. and Treumann, R. A., Basic space plasma physics, Imperial College Press, London, pp. 141–142, 1997.

Cowley, S. W. H., The causes of convection in the Earth's magnetosphere: A review of developments during the IMS, Rev. Geophys. Space Phys., 20, 531–565, 1982.

Dungey, J. W., Interplanetary magnetic fields and the auroral zones, Phys. Rev. Lett., 6, 47–48, 1961.

Eastman, T. E., Hones, Jr., E. W., Bame, S. J., and Asbridge, J. R., The magnetospheric boundary layer: Site of plasma, momentum, and energy transfer from the magnetosheath into the magnetosphere, Geophys. Res. Lett., 3, 685–688, 1976.

Fairfield, D. H., Average and unusual locations of the Earth's magnetopause and bow shock, J. Geophys. Res., 76, 6700–6716, 1971.

Fujimoto, M., Mukai, T., Kawano, H., Nakamura, M., Nishida, A., Saito, Y., Yamamoto, T., and Kokubun, S., Structure of the low-latitude boundary layer: A case study with Geotail data, J. Geophys. Res., 103, 2297–2308, 1998.

Fuselier, S. A., Klumpar, D. M., and Shelley, E. G., Ion reflection and transmission during reconnection at the Earth's subsolar magnetopause, Geophys. Res. Lett., 18, 139–142, 1991.

Fuselier, S. A., Anderson, B. J., and Onsager, T. G., Particle signatures of magnetic topology at the magnetopause: AMPTE/CCE observations, J. Geophys. Res., 100, 11, 805–821, 1995.

Gosling, T. J., Thomsen, M. F., Bame, S. J., Elphic, R. C., and Russell, C. T., Plasma flow reversals at the dayside magnetopause and the origin of asymmetric polar cap convection, J. Geophys. Res., 95 8073–8084, 1990a.

Gosling, J. T., Thomsen, M. F., Bame, S. J., Onsager, T. G., and Russell, C. T., The electron edge of the low latitude boundary layer during accelerated flow events, Geophys. Res. Lett., 17, 1833–1836, 1990b.

Hall, D. S., Chaloner, C. P., Bryant, D. A., Lepine, D. A., and Tritakis, V. P., Electrons in the boundary layers near the dayside magnetopause J. Geophys. Res., 96, 7869–7891, 1991.

Hapgood, M. A. and Bryant, D. A., Re-ordered electron data in the low-latitude boundary layer, Geophys. Res. Lett., 17, 2043–2046, 1990.

Johnstone, A. D., Rodgers, D. J., Coates, A. J., Smith, M. F., and Southwood, D. J., Ion acceleration during steady-state reconnection at the dayside magnetopause, in Ion acceleration in the Magnetosphere and Ionosphere, Geophys. Monogr. Ser., vol. 38, edited by T. Chang, pp. 136–140, AGU, Washington, D. C., 1986.

Le, G., Russell, C. T., Gosling, J. T., and Thomsen, M. F., ISEE observations of low-latitude boundary layer for northward interplanetary magnetic field: Implications for cusp reconnection, J. Geophys. Res., 101, 27, 239–249, 1996.

Levy, R. H., Petschek, H. E., and Siscoe, G. L., Aerodynamic aspects of the magnetospheric flow, AAIA J., 2, 2065–2076, 1964.

Lühr, H., Klöcker, N., Oelschlägel, W., Häusler, B., and Acuña, M., The IRM fluxgate magnetometer, IEEE Trans. Geosci. Remote Sens., GE-23, 259–261, 1985.

Nakamura, M., Teresawa, T., Kawano, H., Fujimoto, M., Hirahara, M., Mukai, T., Machida, S., Saito, Y., Kokubun, S., Yamamoto, T., and Tsurada, K., Leakage ions from the LLBL to MSBL: Confirmation of reconnection events at the dayside magnetopause, J. Geomagn. Geoelec., 47, 65–70, 1996.

Nakamura, M., Fujimoto, M., Kawano, H., Mukai, T., Saito, Y., Yamamoto, T., Tsurada, K., Teresawa, T., and Kokubun, S., Geotail observations at the dayside magnetopause — Confirmation of reconnection events, Adv. Space Res., 20, (4/5), 779–788, 1997.

Nakamura, M., Seki, K., Kawano, H., Obara, T., and Mukai, T., Reconnection event at the dayside magnetopause on 10 January 1997, Geophys. Res. Lett., 25, 2529–2532, 1998.

Ogilvie, K. W., Fitzenreiter, R. J., and Scudder, J. D., Observations of electron beams in the low latitude boundary layer, J. Geophys. Res., 89, 10, 723–732, 1984.

Onsager, T. G. and Fuselier, S. A., The location of magnetopause reconnection for northward and southward interplanetary magnetic field, in Solar System Plasmas in Space and Time, Geophys. Monogr. Ser., vol. 84, edited by Burch, J. and Waite, Jr., J. H., pp. 183–197, AGU, Washington, D. C., 1994.

Paschmann, G., Sonnerup, B. U. Ö., Papamastorakis, I., Sckopke, N., Haerendel, G., Bame, S. J., Asbridge, J. R., Gosling, J. T., Russell, C. T., and Elphic, R. C., Plasma acceleration at the Earth's magnetopause: Evidence for reconnection, Nature, 282, 243–246, 1979.

Paschmann, G., Loidl, H., Obermayer, P., Ertl, M., Laborenz, R., Sckopke, N., Baumjohann, W., Carlson, C. W., and Curtis, D. W., The plasma instrument for AMPTE/IRM, IEEE Trans. Geosci. Remote Sens., GE-23, 262–266, 1985.

Paschmann, G., Papamastorakis, I., Baumjohann, W., Sckopke, N., Carlson, C. W., Sonnerup, B. U. Ö., and Lühr, H., The magnetopause for large magnetic shear: AMPTE/IRM observations, J. Geophys. Res., 91, 11, 099–115, 1986.

Paschmann, G., Sonnerup, B. U. Ö., Papamastorakis, I., Baumjohann, W., Sckopke, N., and Lühr, H., The magnetopause and boundary layer for small magnetic shear: Convection electric fields and reconnection, Geophys. Res. Lett., 17, 1829–1832, 1990.

Paschmann, G., Baumjohann, W., Sckopke, N., Phan, T.-D., and Lühr, H., Structure of the dayside magnetopause for low magnetic shear, J. Geophys. Res., bf 98, 13, 409–422, 1993.

Phan, T.-D., and Paschmann, G., Low-latitude dayside magne-

topause and boundary layer for high magnetic shear: 1. Structure and motion, J. Geophys. Res., 101, 7801–7815, 1996.

Phan, T.-D., Paschmann, G., Baumjohann, W., Sckopke, N., and Lühr, H., The magnetosheath region adjacent to the dayside magnetopause: AMPTE/IRM observations, J. Geophys. Res., 99, 121–141, 1994.

Phan, T.-D., Paschmann, G., and Sonnerup, B. U. Ö., Low-latitude dayside magnetopause and boundary layer for high magnetic shear: 2. Occurrence of magnetic reconnection, J. Geophys. Res., 101, 7817–7828, 1996.

Phan, T.-D., Kistler, L. M., Klecker, B., Haerendel, G., Paschmann, G., Sonnerup, B. U. Ö., Baumjohann, W., Bavassano-Cattaneo, M. B., Carlson, C. W., DiLellis, A. M., Fornacon, K.-H., Frank, L. A., Fujimoto, M., Georgescu, E., Kokubun, S., Moebius, E., Mukai, T., Øieroset, M., Paterson, W. R., and Rème, H., Extended magnetic reconnection at the Earth's magnetopause from detection of bi-directional jets, Nature, 404, 848–850, 2000.

Pottelette, R. and Treumann, R. A., Impulsive broadband electrostatic noise in the cleft: A signature of dayside reconnection, J. Geophys. Res., 103, 9299–9307, 1998.

Puhl-Quinn, P. A. and Scudder, J. D., Systematics of ion Walén analysis of rotational discontinuities using E/Z, J. Geophys. Res., 105, 7617–7627, 2000.

Rijnbeek, R. P., Cowley, S. W. H., Southwood, D. J., and Russell, C. T., A survey of dayside flux transfer events observed by the ISEE-1 and -2 magnetometers, J. Geophys. Res., 89, 786–800, 1984.

Russell, C. T. and Elphic, R. C., Initial ISEE magnetometer results: Magnetopause observations, Space Sci. Rev., 22, 681–715, 1978.

Russell, C. T. and Elphic, R. C., ISEE observations of flux transfer events at the dayside magnetopause, Geophys. Res. Lett., 6, 33–36, 1979.

Sckopke, N., Paschmann, G., Haerendel, G., Sonnerup, B. U. Ö., Bame, S. J., Forbes, T. G., Hones, Jr., E. W., and Russell, C. T., Structure of the low latitude boundary layer, J. Geophys. Res., 86, 2099–2110, 1981.

Scudder, J. D., Theoretical approaches to the description of magnetic merging: The need for finite β_e, anisotropic, ambipolar Hall MHD, Space Sci. Rev., 80, 235–267, 1997.

Scudder, J. D., Puhl-Quinn, P. A., Mozer, F. S., Ogilvie, K. W., and Russell, C. T., Generalized Walén tests through Alfvén waves and rotational discontinuities using electron flow velocities, J. Geophys. Res., 104, 19, 817–833, 1999.

Smith M. F. and Rodgers, D. J., Ion distributions at the dayside magnetopause, J. Geophys. Res., 96, 11, 617–624, 1991.

Song, P., Russell, C. T., Fitzenreiter, R. J., Gosling, J. T., Thomsen, M. F., Mitchell, D. G., Fuselier, S. A., Parks, G. K., Anderson, R. R., and Hubert, D., Structure and properties of the subsolar magnetopause for northward interplanetary magnetic field: Multiple-instrument particle observations, J. Geophys. Res., 98, 11, 319–337, 1993.

Sonnerup, B. U. Ö., Paschmann, G., Papamastorakis, I., Sckopke, N., Haerendel, G., Bame, S. J., Asbridge, J. R., Gosling, J. T., and Russell, C. T., Evidence for magnetic field reconnection at the Earth's magnetopause, J. Geophys. Res., 86, 10, 049–067, 1981.

Sonnerup, B. U. Ö., Papamastorakis, I., Paschmann, G., and Lühr, H., Magnetopause properties from AMPTE/IRM observations of the convection electric field: Method development, J. Geophys. Res., 92, 12, 137–159, 1987.

Sonnerup, B. U. Ö., Papamastorakis, I., Paschmann, G., and Lühr, H., The magnetopause for large magnetic shear: Analysis of convection electric fields from AMPTE/IRM, J. Geophys. Res., 95, 10, 541–557, 1990.

Southwood, D. J., Saunders, M. A., Dunlop, M. W., Mier-Jedrzejowicz, W. A. C., and Rijnbeek, R. P., A survey of flux tranfer events recorded by the UKS spacecraft magnetometer, Planet. Space Sci., 34, 1349–1359, 1986.

Zwan, B. J. and Wolf, R. A., Depletion of solar wind plasma near a planetary boundary, J. Geophys. Res., bf 81, 1636–1648, 1976.